Cationic Imidazolium Macrocycles Enable Array-based, Site-Selective Sensing of Peptide Phosphorylation

Arman C. Garcia, Ria Lian, Parisa Fashihianifard, Lin He, Ryan R. Julian, Veronica Carta, Chia-en A. Chang, and Richard J. Hooley*

Department of Chemistry; University of California-Riverside, Riverside, CA 92521, U.S.A.

E-mail: richard.hooley@ucr.edu

Electronic Supplementary Information

Table of Contents

1. General Information

Chemicals and Reagents

Fluorophores **DSMI**,[1] **DQMI**,[2] **PSMI**,[3] **DTMI**[4] and **SMITE**[5] were synthesized and characterized according to literature procedures. Fluorophores **QR**, **Indigo Carmine**, **Food Yellow 3**, and **Methyl Orange** were purchased and used as received. Methylene-diimidazole (MDI) was prepared according to literature procedures.[6] Protected amino acids, Fmoc-Glu(otbu)-OH, Fmoc-Leu-OH, Fmoc-Lys(Boc)-OH, Fmoc-Trp(boc)-OH, Fmoc-O-(benzylphospho)-L-Serine, Ethyl cyanoglyoxylate-2-oxime (oxyma) were purchased from Combi-Blocks. Protected amino acids such as Fmoc-L-isoleucine, Fmoc-Arg(pbf)-OH, Fmoc-L-isoleucine, and Rink amide MBHA resin were purchased from Ambeed. 1,4-Bis(bromomethyl)benzene was purchased from TCI Chemicals. 3-Bromo-2-(bromomethyl)propionic acid and 3-Bromo-2-(bromomethyl)prop-1-ene were purchased from Enamine.

The pyrogen-, nuclease- and bacteria-free ultrapure (Type 1) water produced by Direct-Q 3 UV water purification system with Biopak polisher (Catalog Number CDUFBI001), was used in peptide experiments. The Wdfy3 peptides purified by HPLC were purchased from Biomatik, the sequence modification of which is given in Table *S*-4. The concentrations of peptide stock solutions were measured by the NanoDrop 2000 (Thermo Fisher Scientific) using the corresponding molar extinction coefficients at 280 nm in water calculated by the Expasy ProtParam tool (https://web.expasy.org/protparam/) after background subtraction. The pH values of solutions were measured by Fisher Scientific Accumet Excel XL50 Dual Channel pH/Ion/Conductivity Meter with Fisherbrand Accumet glass body standard size combination electrode, which was pre-calibrated using RICCA Chemical pH buffer reference standard solutions of pH 4.00, 7.00, and 10.00. Solvents were dried through a commercial solvent purification system (Pure Process Technologies, Inc.).

^{1}H and ^{13}C NMR spectra were recorded on Bruker Avance NEO 400 MHz and 600 MHz NMR spectrometer. The spectrometers were automatically tuned and matched to the correct operating frequencies. Proton (^{1}H) and carbon (^{13}C) chemical shifts are reported in parts per million (d) with respect to tetramethylsilane (TMS, d = 0) and referenced internally with respect to the protio solvent impurity. Deuterated NMR solvents were obtained from Cambridge Isotope Laboratories, Inc., Andover, MA, and used without purification. High-resolution accurate mass spectral data

were obtained from the Analytical Chemistry Instrumentation Facility at the University of California, Riverside, on an Agilent 6545 Q-TOF LC/MS instrument. Mass spectra of **PTI•Br** were acquired on a Thermo Fisher Scientific LTQ mass spectrometer and a Thermo Scientific Orbitrap Fusion Lumos. Samples were introduced via a Thermo Scientific Nanoflex source, which was modified with a platinum wire to accommodate nanospray tips pulled from borosilicate glass capillaries (Harvard Apparatus GC100T-10). The nanospray emitters had tip diameters of approximately ~1-15 um in diameter and a taper length of ~1 mm. Prior to analysis, **PTI•Br** was reconstituted and diluted to 10 μM in Optima-grade water. For LTQ analysis, the instrument was tuned on the **PTI•Br** complex and ions were detected in the ion trap. For Orbitrap Fusion Lumos measurements, data were collected at 120,000 resolving power (at m/z 200) using 10 scans of 10 microscans each.

Solid-phase Peptide Synthesis and Purification of 13-Amino Acid Peptides

Peptides (Ptpn13 WT and Ptpn13 Sp7) were synthesized on a 0.1 mmol/g scale using a CSBIO II synthesizer. For the coupling step, *N*,*N'*-diisopropylcarbodiimide (DIC) (0.4 M) was used as an activating reagent, while 20% 4-methylpiperidine (PIP) in DMF serves as a deprotection solution. DMF was used as the main solvent throughout the process, and the temperature was kept at 90°C. Each protected amino acid was weighed and dissolved in 2.5 mL of 0.4 M oxyma in DMF, where oxyma functioned as an additive to minimize racemization during coupling.[7] Pre-swelled Rink amide MBHA resin was used and transferred to the reaction vessel. After the synthesis, the final deprotection was carried out by mixing the resin in 5 mL of 20% PIP in DMF solution and was mixed for 20 minutes. Then the resin was washed with DMF to remove excess PIP, followed by CH_2Cl_2 to remove DMF. The deprotected resin was then dried under vacuum prior to the cleavage step. The initial cleavage process began by stirring the dried resin in a mixture of 9.5:2.5:2.5 of TFA/triisopropyl silane/H_2O for 2 hours. The resin was filtered under vacuum and washed with CH_2Cl_2. The filtrate was collected, and excess solvent was removed by rotary evaporation. The concentrated filtrate was transferred to a centrifuge tube and cold ether was added to precipitate the peptide. The mixture was centrifuged for 5 mins, and the precipitate was collected. The resulting pellet was washed several times with cold ether by resuspension, centrifugation, and removal of the supernatant. Lastly, the resulting peptide was dried under vacuum.

The crude peptides were purified on a Dionex UltiMate 3000 system equipped with a variable-wavelength detector, using a Kinetex EVO C18 column (5 μM, 100 Å, 250 x 21.2 mm, AXIA packed). General HPLC conditions were as follows: Solvent A (H_2O with 0.1% TFA) and Solvent B (MeCN with 0.01% TFA) at a flow rate of 5 mL/min. The gradient began at 85% Solvent A at 0 min, decreased to 50% at 25 min, and was then transitioned to 0% Solvent A. Data acquisition was performed using Chromeleon 7 software.

The MS and MS/MS spectra were obtained using AB SCIEX 5800 matrix-assisted laser desorption ionization time-of-flight (MALDI-TOF) mass spectrometer. Samples were prepared by mixing 0.75 L of each collected fraction with 2.5 μL of matrix solution. The matrix solution was prepared by dissolving α-Cyano-4-hydroxycinnamic acid (CHCA) to saturation in a 1:1 mixture of MeCN and H_2O with 0.1% TFA. The samples were then spotted onto a stainless- steel Opti-TOF 96-target plate and allowed to dry prior to analysis. Ptpn13 WT, $C_{69}H_{114}N_{18}O_{22}$, $[M+H]^+$ calculated 1547.84, found 1546.70. Ptpn13 Sp7, $C_{69}H_{115}N_{18}O_{25}P$, $[M+H]^+$ calculated 1627.84, found 1626.76. After MS characterization, excess solvent from the fractions was removed by lyophilization.

X-ray Crystallography

PTI•PF_6 (10 mg, 0.001 mmol)) was dissolved into 500 μL of CH_3CN. Tetrabutylammonium bicarbonate (1.8 mg, 0.01 mmol, 10 equiv.) was dissolved to 100 μL of CH_3CN and added dropwise to the solution of **PTI•**PF_6. A white precipitate formed and was subsequently filtered off. The resulting filtrate was treated to vapor diffusion of diisopropyl ether, producing suitable crystals for X-Ray analysis after 3 days. A colorless crystal (plate, approximate dimensions 0.48 × 0.1 × 0.05 mm3) was placed onto the tip of a MiTeGen pin and mounted on a Bruker Venture D8 diffractometer equipped with a PhotonIII detector at 100.0 K. The data collection was carried out using Cu Ka radiation (l = 1.54178 Å, ImS micro-source) with a frame time of 6 seconds and a detector distance of 40 mm. A collection strategy was calculated and complete data to a resolution of 0.82 Å were collected. The frames were integrated with the Bruker SAINT[8] software package using a narrow-frame algorithm to 0.82 Å resolution. Data were corrected for absorption effects using the multi-scan method (SADABS).[9] Please refer to Table *S*-1 for additional crystal and refinement information.

Structure Solution and Refinement

The space group P*bca* was determined based on intensity statistics and systematic absences. The structure was solved using the SHELX suite of programs[10,11] and refined using full-matrix least-squares on F^2 within the OLEX2 suite.[12] An intrinsic phasing solution was calculated, which provided most non-hydrogen atoms from the E-map. Full-matrix least squares /difference Fourier cycles were performed, which located the remaining non-hydrogen atoms. All non-hydrogen atoms were refined with anisotropic displacement parameters. The hydrogen atoms were placed in ideal positions and refined as riding atoms with relative isotropic displacement parameters. Disorder was modeled for the PF_6 anions and for the acetonitrile molecules. The final full matrix least squares refinement converged to $R1 = 0.0896$ and $wR2 = 0.2182$ (F^2, all data). The goodness-of-fit was 1.076. On the basis of the final model, the calculated density was 1.481 g/cm^3 and $F(000)$, 4670.

1.1 Chemical Synthesis and Characterization

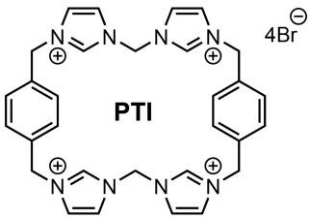

Synthesis of PTI•Br

To a one-necked round-bottomed flask was equipped with a stir bar and di(1H-imidazol-1-yl)methane (100 mg, 0.67 mmol), and 100 mL of acetonitrile. 1,4-Bis(bromomethyl) benzene (195 mg, 0.74 mmol) was dissolved in 50 mL of acetonitrile and dropwise over a 6-hour period via syringe pump. Upon completion the reaction mixture was refluxed for 48 h. After heating, the reaction mixture was allowed to cool at ambient conditions and briefly sonicated. The mixture was then filtered via vacuum filtration and rinsed with excess acetonitrile and dried under high vacuum to a white powder (110 mg, 40%). Note that **PTI•Br** exists as a 1:1 mixture of monomer and dimer species in water. ^{1}H NMR (600 MHz, DMSO-d_6) δ 9.63 (s, 4H), 8.11 (s, 4H), 7.89 (s, 4H), 7.51 (s, 8H), 6.69 (s, 4H), 5.48 (s, 8H) ^{13}C {^{1}H} NMR (400 MHz, DMSO-d_6) δ 137.9, 134.9, 130.2,

123.5, 58.3, 52.3 HRMS (nESI-Orbitrap) *m/z* $[M]^{4+}$ Calcd for $C_{30}H_{32}N_8$ 126.0682; Found 126.0682 Monomer: (600 MHz, D_2O) δ 9.18 (s, 1H)*, 7.84 (s, 4H), 7.70 (s, 4H), 7.50 (s, 8H), 6.60 (s, 4H), 5.41 (s, 8H) Dimer: (600 MHz, D_2O) δ 9.36 (s, H)*, 7.77 (s, 4H), 7.58 (s, 4H), 7.48 (s, 8H), 6.60 (s, 4H), 5.41 (s, 8H) ^{13}C {^1H} NMR (400 MHz, D_2O) δ 136.4, 133.7, 132.8, 130.9, 129.8, 124.0, 123.7, 122.4, 58.9, 58.3, 53.1, 53.0. *Denotes proton that undergoes H-D exchange.

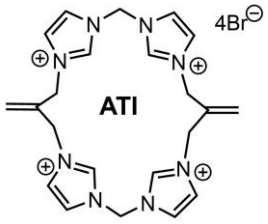

Synthesis of ATI•Br

To a one-necked round-bottomed flask was equipped with a stir bar and di(1H-imidazol-1-yl)methane (100 mg, 0.67 mmol), and 100 mL of acetonitrile. 3-Bromo-2-bromomethyl-1-propene (78 μL, 0.74 mmol) was dissolved in 45 mL of acetonitrile and dropwise over a 6-hour period via syringe pump. Upon completion the reaction mixture was allowed to reflux for 3 days resulting in a white precipitate. After heating, the reaction mixture was allowed to cool at ambient conditions and briefly sonicated. The mixture was then filtered by vacuum filtration and rinsed with excess acetonitrile and dried under high vacuum (43 mg, 8.9%). Note that **ATI•Br** exists as a 1:1 mixture of monomer and dimer species in water.^1H NMR (600 MHz, DMSO-d_6) δ 9.72 (s, 4H), 7.79 (s, 4H), 7.76 (s, 4H), 6.59 (s, 4H), 5.90 (s, 4H), 5.00 (s, 8H) $^{13}C\{^1H\}$ NMR (400 MHz, D_2O) δ 134.6, 132.5, 131.2, 124.2, 124.0, 122.6, 121.8, 58.9, 53.6, 51.5 HRMS (ESI-TOF) *m/z* $[M]^{4+}$ Calcd for $C_{22}H_{28}N_8$ 101.0604; Found 101.0604 ^1H NMR (600 MHz, D_2O) δ 7.81 (s, 4H), 7.67 (s, 4H), 7.60 (s, 4H), 7.54 (s, 4H), 7.53 (s, 4H), 6.69 (s, 4H), 6.54 (s, 4H), 5.94 (s, 4H), 5.31 (s, 4H), 5.07 (s, 8H), 4.93 (s, 8H).

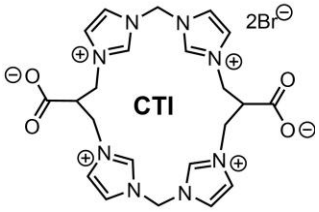

Synthesis of CTI•Br

To a one-necked round-bottomed flask was equipped with a stir bar and di(1H-imidazol-1-yl)methane (100 mg, 0.67 mmol), and 100 mL of acetonitrile. 3-Bromo-2-(bromomethyl)propionic acid (170 mg, 0.74 mmol) was dissolved in 50 mL of acetonitrile and dropwise over an 8-hour period via syringe pump. The reaction mixture was refluxed for 4 days upon a white solid was produced. The reaction mixture was allowed to at ambient conditions and the solvent was decanted. 10 mL of water was added to the round bottom flask and collected into a scintillation vial and concentrated down to a light blue oil. (140 mg, 67%). Note that **CTI•Br** exists as a 9:1 mixture of monomer and dimer species in water. ^{1}H NMR (600 MHz, D_2O) Monomer: δ 9.23 (s, 1H)*, 7.83 (s, 4H), 7.78 (s, 4H), 6.76 (s, 4H), 4.65 (s, 8H), 3.63 (s, 2H) Dimer: δ 9.43 (s, 1H)*, 7.79 (s, 4H), 7.58 (s, 4H), 6.76 (s, 4H), 4.65 (s, 8H), 3.63 (s, 2H) *Denotes proton that undergoes H-D exchange. ^{13}C {^{1}H} NMR (400 MHz, D_2O) δ 173.1, 138.0, 136.3, 124.2, 122.4, 121.5, 121.2, 59.0, 58.9, 48.8, 47.2 HRMS (ESI-TOF) *m/z* $[M]^{2+}$ Calcd for $C_{22}H_{26}N_8O_8$ 233.1033; Found 233.1021.

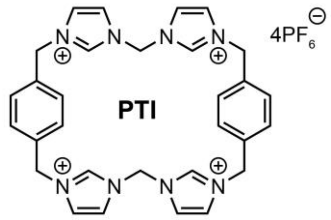

Synthesis of PTI•PF$_6$

To a one-neck round bottom flask was equipped with a stir bar and **PTI•Br** (100 mg, 0.112 mmol) and dissolved into 5 mL of water. Ammonium hexafluorophosphate (199 mg, 1.22 mmol) was dissolved in 5 mL of water and added dropwise to the solution of **PTI•PF$_6$**. The mixture was allowed to stir overnight and was filtered via vacuum filtration and rinsed with excess water. The white solid was collected and dried over high vacuum to a white powder (74 mg, 68%). ^{1}H NMR (600 MHz, CD_3CN) δ 9.01 (s, 4H), 8.86 (s, 4H), 7.69 (s, 4H), 7.62 (s, 4H), 7.49 (s, 4H), 7.48 (s,

8H), 7.45 (s, 4H), 7.44 (8H), 6.45 (s,4H), 6.38 (s, 4H), 5.40 (s, 8H), 5.35 (8H) ^{13}C {^{1}H} NMR (400 MHz, CD_3CN) δ 138.0, 137.8, 135.0, 134.5, 131.0, 130.5, 124.4, 124.0, 123.6, 59.8, 59.1, 53.7, 53.6 HRMS (ESI-TOF) *m/z* $[M]^{2+}$ Calcd for $C_{30}H_{32}N_8O_8P_2F_{12}$ 397.1012; Found 397.1004.

Table S-1 Crystal data and structure refinement for $[C_{30}H_{32}N_8Cl][PF_6]$ (CCDC 2501030).

Formula	$C_{37.79}H_{44.92}ClF_{17.95}N_{11.90}O_{0.66}P_3$
Formula weight	1145.85
Temperature	100.0 K
Wavelength, Å	1.54178
crystal system, space group	Orthorhomic
space group	*Pbca*
a, Å	16.0418(7)
b, Å	24.9817 (12)
c, Å	25.6422 (11)
α, °	90°
β, °	90°
γ, °	90°
Volume	10276.1(8) $Å^3$
Z,	8
Calculated density, mg/m^3	1.481
Absorption coeffecient, mm^{-1}	2.528
F(000)	4670
Crystal size, mm	Colorless plate 0.48 × 0.1 × 0.005
Theta range for data collection, deg	3.70 to 70.144
Limiting indices	-19<=h<=19, -30<=k<=30, -27<=l<=31
Reflections collected / unique	184116, 9767 [R_{int} = 0.0946]
Completeness to θ = 67.679°	99.9%
Absorption correction	Semi-empirical from equivalents
Refinement method	Full-matrix least-squares on F^2
Data / restraints / parameters	9767 192 / 712
Goodness-of-fit on F^2	1.076
Final *R* indices [I > 2σ(*I*)]	*R*1 =0.0896, *wR*2 = 0.2141
R indices (all data)	*R*1 =0.0953, *wR*2 = 0.2182
Largest diff. Peak and hole, e $Å^3$	0.833, -0.660

1.2 Fluorescence Measurements

Fluorescence measurements were performed using two instruments: the BioTek Synergy H1 Hybrid Multi-Mode Microplate Reader and the Agilent BioTek Synergy H1 Multi-Mode Microplate Reader, both operated in Fluorescence Endpoint mode. Excitation/emission wavelength settings were as follows: 480/600 nm (**DSMI**), 500/600 nm (**PSMI**), 540/600 nm (**DTMI**), 528/630 nm (**QR**), 530/640 nm (**DQMI**), 462/528 nm (**Methyl Orange**), 380/560 nm (**SMITE**), 600/630 nm (**Indigo Carmine**), and 480/570 nm (**Food Yellow 3**). On the Agilent instrument, gain was individually optimized for each dye: 126 (**DSMI**), 100 (**DTMI**), 140 (**QR**), 119 (**PSMI**), 150 (**DQMI**), 120 (**Methyl Orange**), 100 (**SMITE**), and 150 (**Indigo Carmine** and **Food Yellow 3**). The BioTek instrument was run with a fixed gain of 100 and was used to measure **XTI** (**PTI•Br**, **CTI•Br**, and **ATI•Br**) and Ptpn13 peptides (WT and Sp7) titrations; all other fluorescence titrations were performed on the Agilent instrument. Fluorescence data were collected using Gen5 software (version 2.09 for the BioTek reader and version 3.16 for the Agilent reader).

XTI:Dye Titrations

The dye stock solutions were prepared in DMSO purchased from Fisher Chemicals at a concentration of 20 mM and later diluted with water for use in experiments. The **XTI** (**PTI•Br**, **CTI•Br**, and **ATI•Br**) stock solutions were also prepared in water and later diluted with water for use in experiments. The fluorescence titration curves were generated by using 0.5 μM **dye** with increasing **XTI** (**PTI•Br**, **CTI•Br**, and **ATI•Br**) concentrations from 0-20 μM. The titration was done in two different buffers: 20 mM Tris-HCl buffer at pH 7.4 and 20 mM free Tris buffer at pH 10.2.

XTI:Dye Affinity in Tris-HCl Buffer

Dissociation constant (K_d) was calculated from XTI-Dye titration experiments. The K_d values were determined using the Supramolecular.org BindFit website[13] assuming a 1:1 binding model for analysis.

Salt Effect on **DSMI** and **PTI•Br** Binding

The fluorescence titration curves were generated by using 0.5 μM **DSMI** with increasing **PTI•Br** concentrations from 0-20 μM. The experiment is done in three different salt (NaCl, NaBr, and NaI) solutions at 500 mM concentration. And another titration experiment was also done in water as a control. The K_d was then calculated and tabulated in Table S-3.

XTI:Peptide Titrations

The fluorescence titration curves were generated by using 2 μM Wdfy3 peptides (WT, Sp3, Sp7, and Sp3Sp7) and Ptpn13 peptides (WT and Sp7) with increasing **XTI (PTI•Br**, **CTI•Br**, and **ATI•Br)** concentrations from 0-20 μM in 20 mM Tris-HCl buffer at pH 7.4.

Differential Sensing Array

The sensing array experiment was conducted using 16 Host:Guest elements, consisting of 0.5 μM dye (**DSMI**, **PSMI**, **DTMI**, and **QR**) and 4 μM or 1 μM of **XTI** (**PTI•Br** and **ATI•Br**) in 20 mM Tris-HCl buffer at pH 7.4. A blank sample was also prepared to calculate the normalized fluorescence response (F/F_0). The sample mixtures were incubated for 20 mins then 100 μL of each mixture was transferred to a 96-well plate. For each of the six peptide targets, five replicate measurements were pipetted into separate wells. The resulting F/F_0 were then inputted into SVM-RFECV and 5 best elements were selected. A t-SNE visualization was performed for the 16 elements, 12 elements, 3 elements and dyes only.

Quantification and Statistical Analysis

The fluorescence emission and F/F_0 bar plots, as well as titration curves were generated with GraphPad Prism 10.6.1. All samples were measured with 3 or 5 repeats, and the average values and standard deviations were reported. Feature selection and classification were performed with Python 3.9 (64-bit), using StandardScaler for data standardization, Recursive Feature Elimination with Cross-Validation (RFECV) to select the optimal subset of features, Support Vector Machine (SVM) (kernel='linear') as the supervised classification estimator, RFECV(estimator=svm.SVC(kernel='linear'), step=1, cv=StratifiedKFold(n_splits=4, shuffle=True), scoring='accuracy', min_features_to_select=1). Performance metrics for the classification evaluation were calculated by using RepeatedStratifiedKFold (n_splits=4, n_repeats=3) for cross validation. The correlation heatmap of selected features was computed

using pandas. DataFrame.corr(method='pearson'). Dimensionality reduction was performed using t-distributed Stochastic Neighbor Embedding (t-SNE) in Python 3.9 (64-bit) to visualize the high-dimensional fluorescence profile. The dataset was standardized using StandardScaler prior to applying t-SNE to ensure uniform scaling of features. The t-SNE algorithm was configured with 2 components for 2D visualization, a perplexity of 5 to balance local and global data relationships, and 10,000 iterations for convergence optimization (TSNE(n_components=2, perplexity=5, n_iter=10000)). The resulting t-SNE embeddings were visualized as scatter plots with density estimates using kernel density estimation (KDE), with contour levels set to 10 to illustrate regions of varying data density. The 3D scatter plot was generated to visualize the distribution of selected features for Wdfy3 and Ptpn13 peptides by using the matplotlib library with a 3D projection.

1.3 Molecular Dynamics Simulations and Interaction Energy Calculations

Molecular dynamics (MD) simulations were conducted using the Amber20 package with GPU acceleration. Initial MD simulations were performed on the apo peptide structures using the ff14IDPs force field to examine peptide flexibility upon phosphorylation. The k-means clustering method was then applied to identify the most populated conformations of the apo structures. These representative conformations were subsequently used for further MD simulations of all apo peptide variants with the ff14SB force field and of **PTI** with the GAFF2 force field.[14,15] The ligand (**PTI**) was parameterized using Amber's Antechamber program with the AM1-BCC partial charge assignment method.[16] Each system was solvated in a rectangular box of explicit TIP3P water extending 12 Å beyond the solute boundaries, and counterions were added to neutralize the overall charge (2 Na^+ for wtwdfy3, 4 Na^+ for sp3wdfy3 and sp7wdfy3, and 6 Na^+ for sp3sp7wdfy; 4 Cl^- ions were added to neutralize the apo **PTI** system).

Energy minimization was carried out in four stages. First, hydrogen atoms, protein sidechains, and the entire protein were minimized sequentially in Generalized Born (GB) implicit solvent[17] for 500, 1,000, and 5,000 steps, respectively, followed by 10,000 steps of water minimization. The entire solvated system was then minimized for 20,000 steps. A 12 Å cutoff was used for direct nonbonded interactions, and long-range electrostatics were treated with the particle mesh Ewald (PME) method.[18] All bonds involving hydrogen were constrained using the SHAKE algorithm, with a 2 fs integration timestep.

Systems were equilibrated in the isothermal–isobaric (NPT) ensemble using a Langevin thermostat. The temperature was gradually increased from 50 to 275 K in 25 K increments (100 ps each), followed by equilibration at 298 K for 2 ns. Production simulations were then performed at 298 K for 500 ns, repeated three times with different random seeds, saving frames every 1 ps (yielding 500,000 frames per run).

Peptide–**PTI** complexes were subsequently constructed in the Molecular Operating Environment (MOE) software, with **PTI** manually positioned near the peptide binding interface. Thereafter, all peptide variants and **PTI** were modeled using the ff14SB and GAFF2 force fields, respectively. Ligand parameterization, solvation (TIP3P water box extending 12 Å), and charge neutralization (2 Cl^- for the wild-type complex and 2 Na^+ for the double-phosphorylated complex) were

performed as described above, followed by standard minimization, equilibration, and production MD simulations.[19]

For analysis of the molecular conformations, each raw trajectories for apo and complex for all variants were resaved every 100 ps using Amber's cpptraj[20] for evaluating intermolecular attractions between ligand and all different peptide variants using the molecular mechanics/Poisson-Boltzmann surface area (MM/PBSA) 3 trajectories method.[21] This method computes the energy (E) of apo system from the apo peptide, and apo **PTI** trajectories, as well as peptide•**PTI** complex separately. The interaction energy was manually calculated for all variants as $D < E > = < E_{complex} > - < E_{peptide} > - < E_{PTI} >$. $< E >$ denotes the computed average energy from a given MD trajectory. The exterior dielectric constant was set to 15 to accommodate the polar protein residues at the protein-water interface. After careful analysis, the most favorable conformations based on energy were picked and optimized afterward.

PTI-DSMI complex with Cl^-: The **PTI–DSMI** complex was prepared using the MOE software. Partial charges for **PTI** and **DSMI** were calculated using the AM1-BCC method, and the GAFF2 force field was applied to the **PTI**–**DSMI** system. The complex was solvated in a TIP3P water box in a rectangular box of explicit water, extending 12 Å beyond the solute edges, 4 Cl^- counterions to neutralize the overall system charge. The complex was minimized with MD simulation standard as described above. The system gradually heated from 50 K to 300 K in increments of 25 K, with each temperature step simulated for 200 ps using a 2 fs time step. Subsequently, the system was equilibrated at 298 K for 500 ps with all atoms relaxed, followed by a 50 ns molecular dynamics production run.

1.4 Data Analysis

The fluorescence emission and F/F_0 bar plots, as well as titration curves were generated with GraphPad Prism 10.6.1. All samples were measured with 3 or 5 repeats, and the average values and standard deviations were reported. Feature selection and classification were performed with Python 3.9 (64-bit), using StandardScaler for data standardization, Recursive Feature Elimination with Cross-Validation (RFECV) to select the optimal subset of features, Support Vector Machine (SVM) (kernel='linear') as the supervised classification estimator, RFECV(estimator=svm.SVC(kernel='linear'), step=1, cv=StratifiedKFold(n_splits=4, shuffle=True), scoring='accuracy', min_features_to_select=1). Performance metrics for the

classification evaluation were calculated by using RepeatedStratifiedKFold (n_splits=4, n_repeats=3) for cross validation. The correlation heatmap of selected features was computed using pandas. DataFrame.corr(method='pearson'). Dimensionality reduction was performed using t-distributed Stochastic Neighbor Embedding (t-SNE) in Python 3.9 (64-bit) to visualize the high-dimensional fluorescence profile. The dataset was standardized using StandardScaler prior to applying t-SNE to ensure uniform scaling of features. The t-SNE algorithm was configured with 2 components for 2D visualization, a perplexity of 5 to balance local and global data relationships, and 10,000 iterations for convergence optimization (TSNE(n_components=2, perplexity=5, n_iter=10000)). The resulting t-SNE embeddings were visualized as scatter plots with density estimates using kernel density estimation (KDE), with contour levels set to 10 to illustrate regions of varying data density. The 3D scatter plot was generated to visualize the distribution of selected features for Wdfy3 and Ptpn13 peptides by using the matplotlib library with a 3D projection.

2. NMR Data

2.1 NMR Characterization of New Molecules

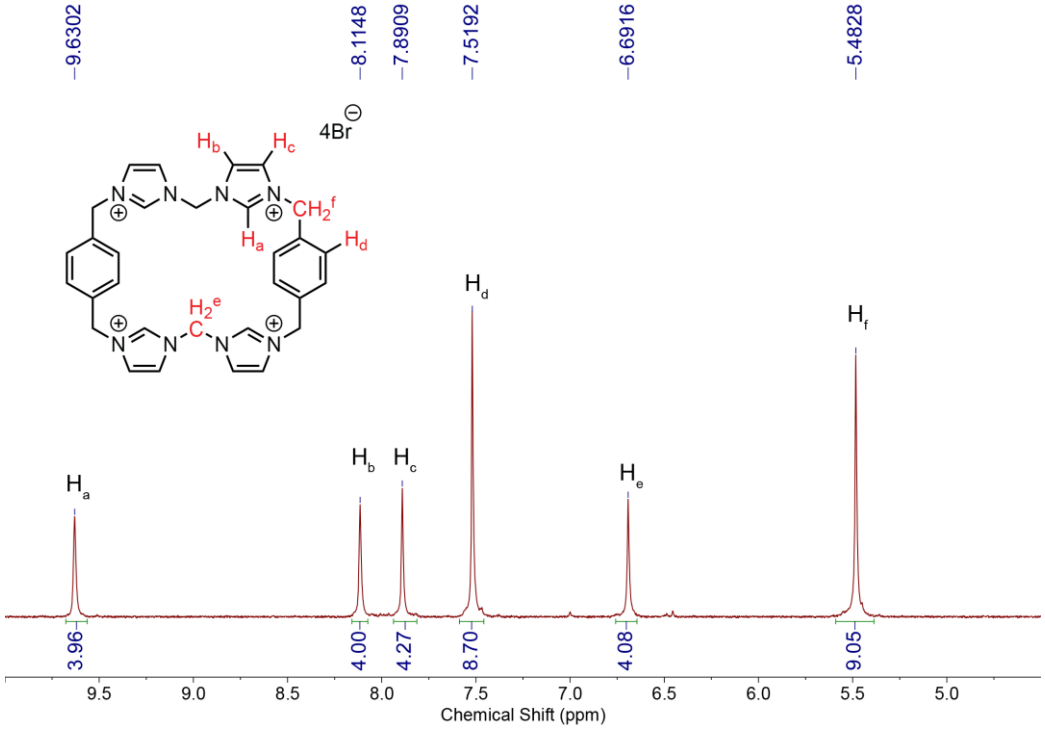

Figure S-1. ^{1}H NMR spectrum of **PTI•Br** (DMSO-d_6, 600 MHz, 298K).

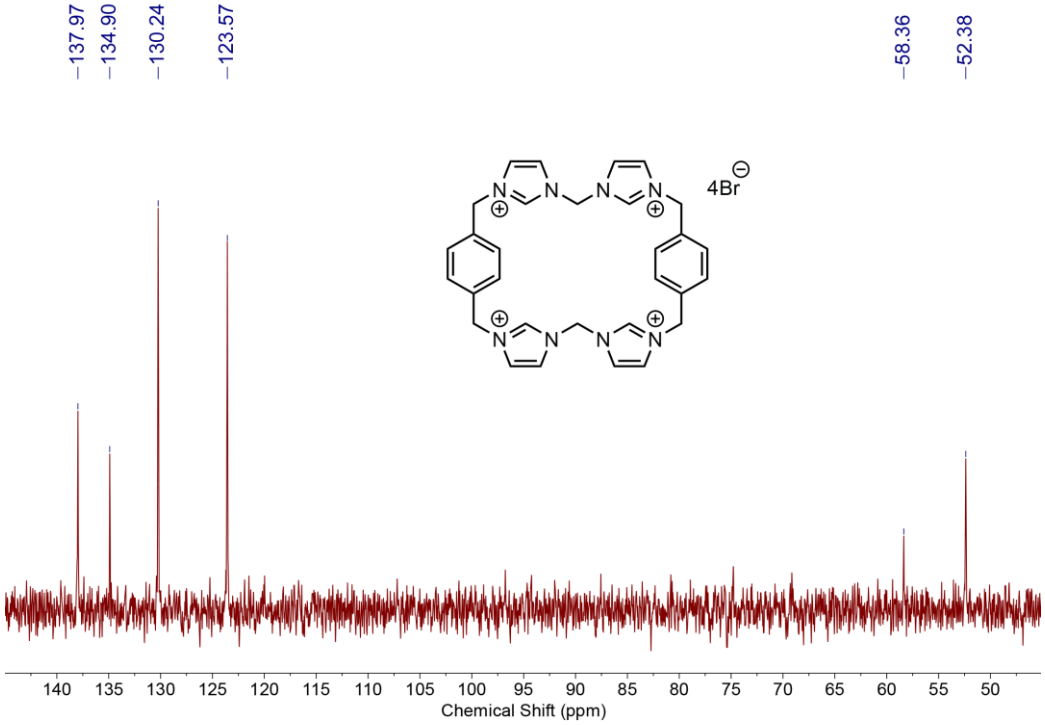

Figure S-2. ^{13}C{^{1}H} NMR spectrum of **PTI•Br** (DMSO-d_6, 101 MHz, 298K).

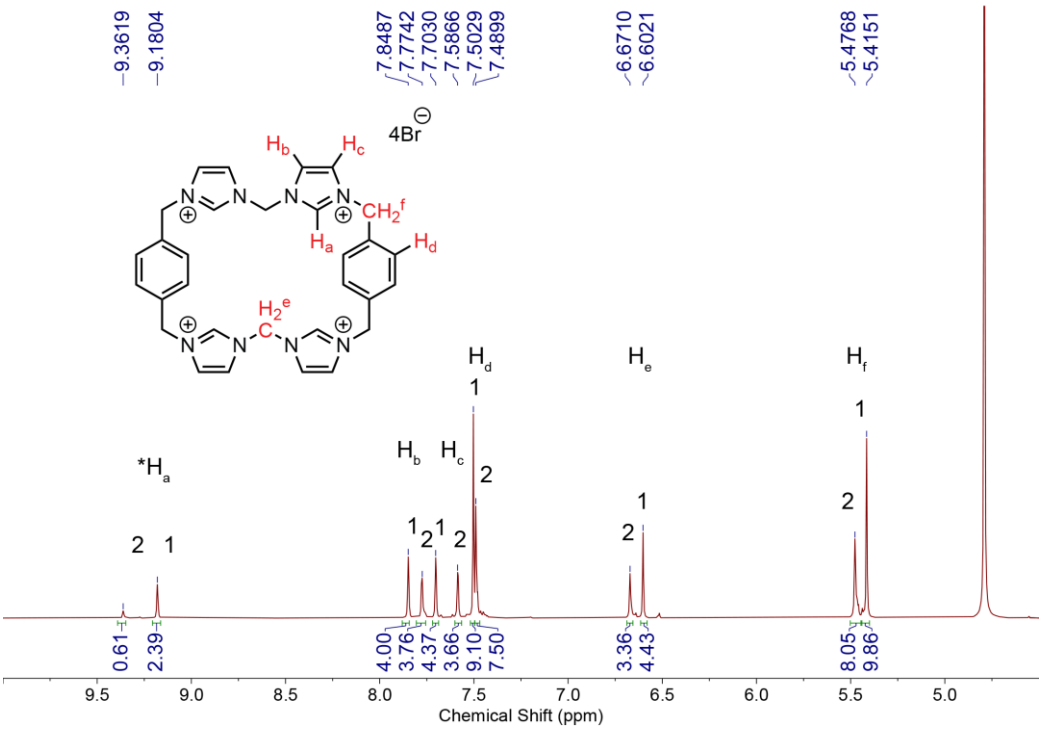

Figure S-3. ^{1}H NMR spectrum of **PTI•Br** (D_2O, 600 MHz, 298K). * Denotes proton that undergoes H-D exchange.

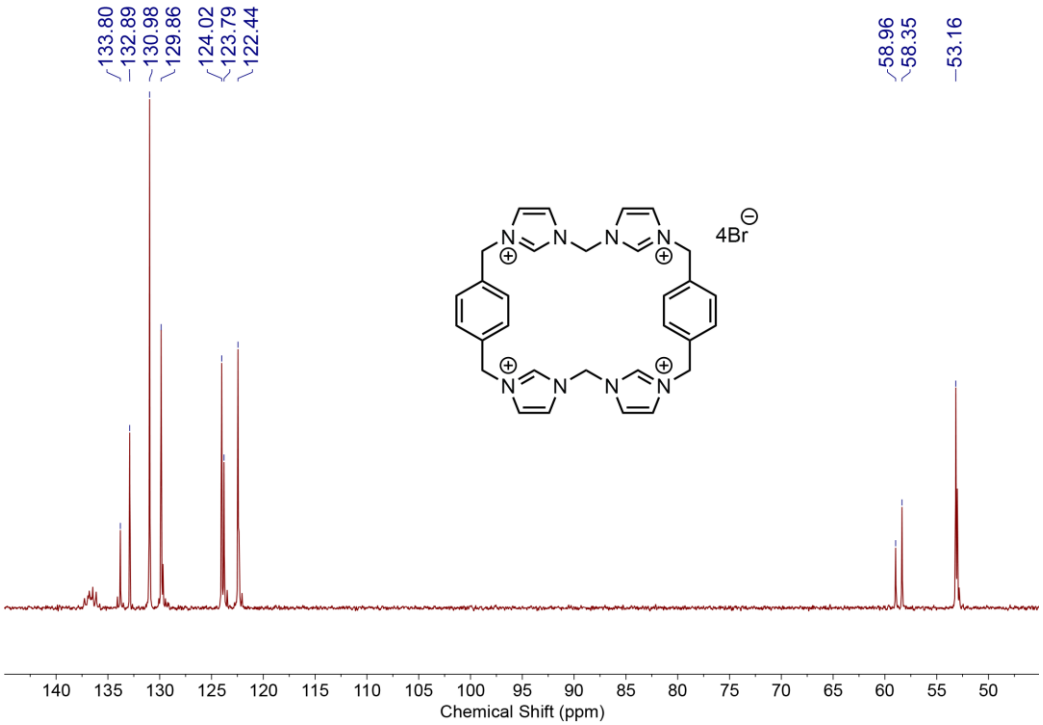

Figure S-4. ^{13}C{^{1}H} NMR spectrum of **PTI•Br** (D_2O, 101 MHz, 298K).

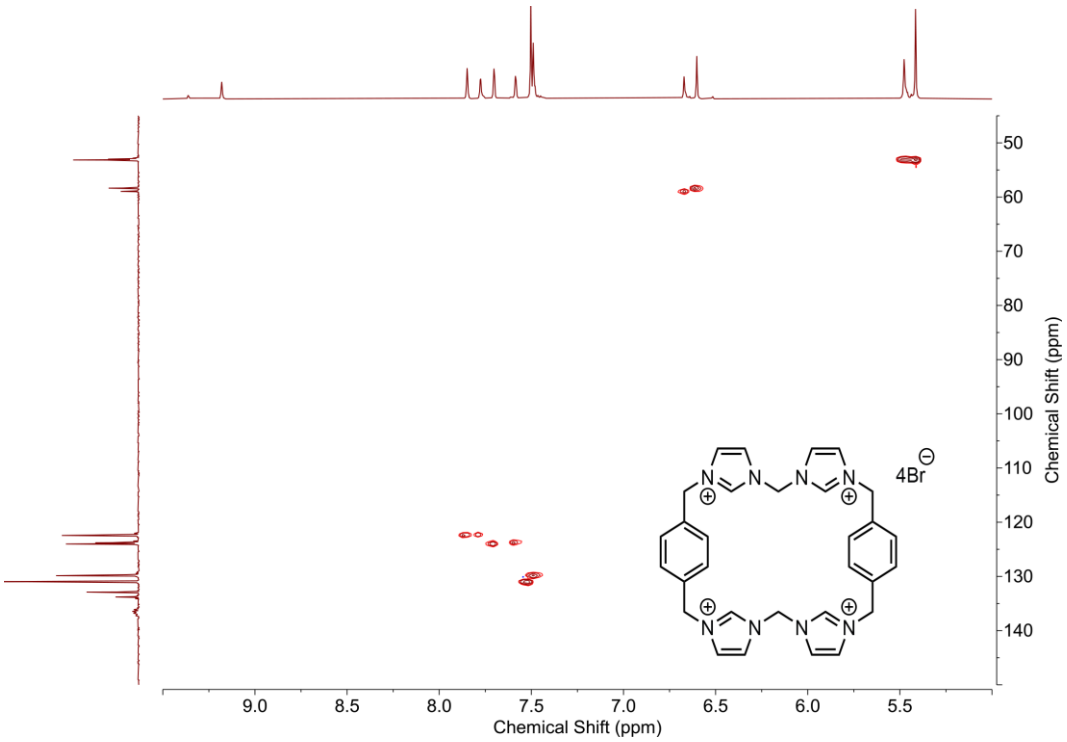

Figure S-5. HSQC NMR spectrum of **PTI•Br** (D_2O, 600 MHz, 298K).

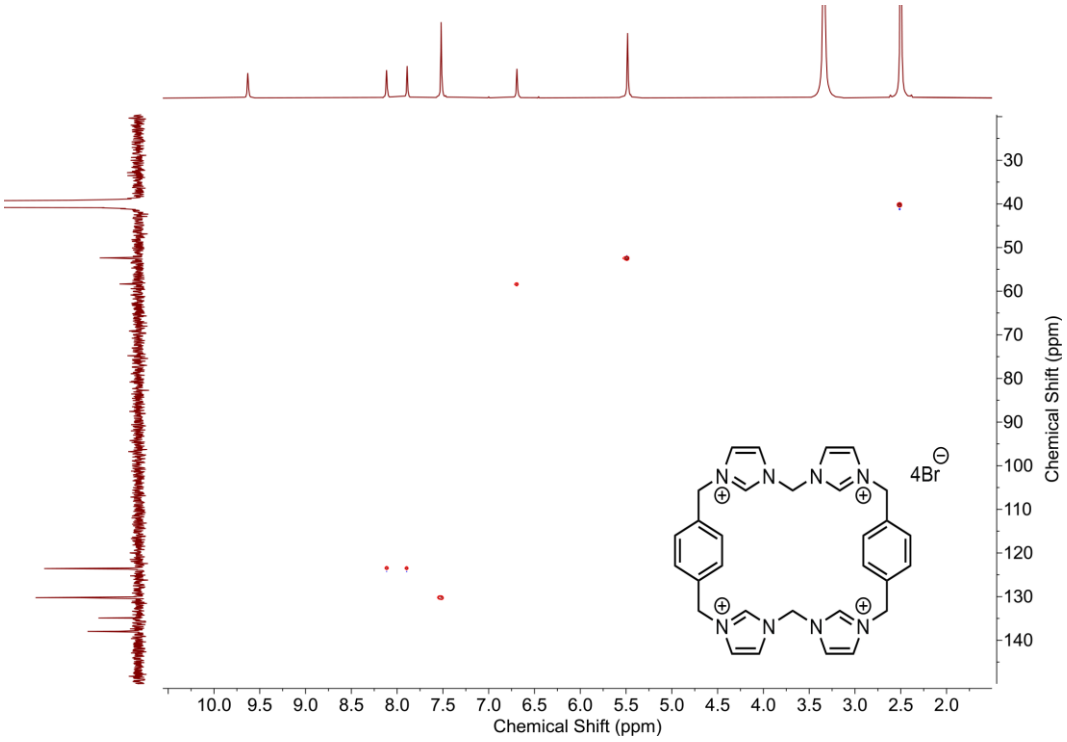

Figure S-6. HSQC NMR spectrum of **PTI•Br** (DMSO-d_6, 600 MHz, 298K).

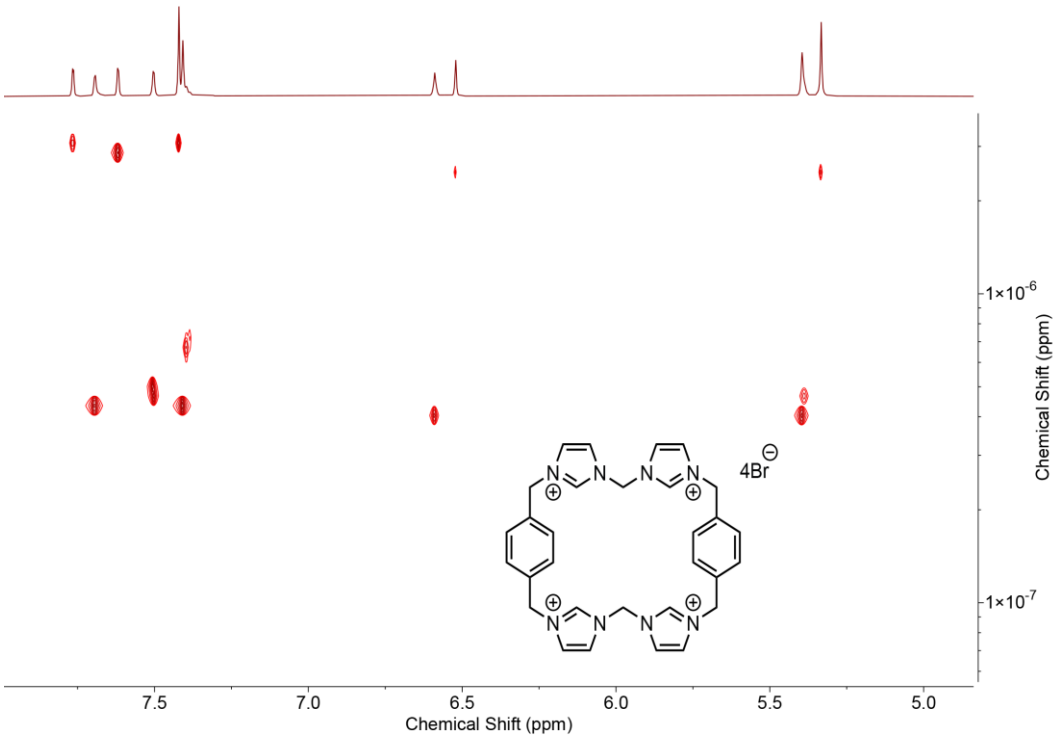

Figure S-7. DOSY NMR spectrum of **PTI•Br** (D_2O, 600 MHz, 298K). Diffusion constant 2.87 x 10^{-7} cm^2/sec and 4.37 x 10^{-7} cm^2/sec.

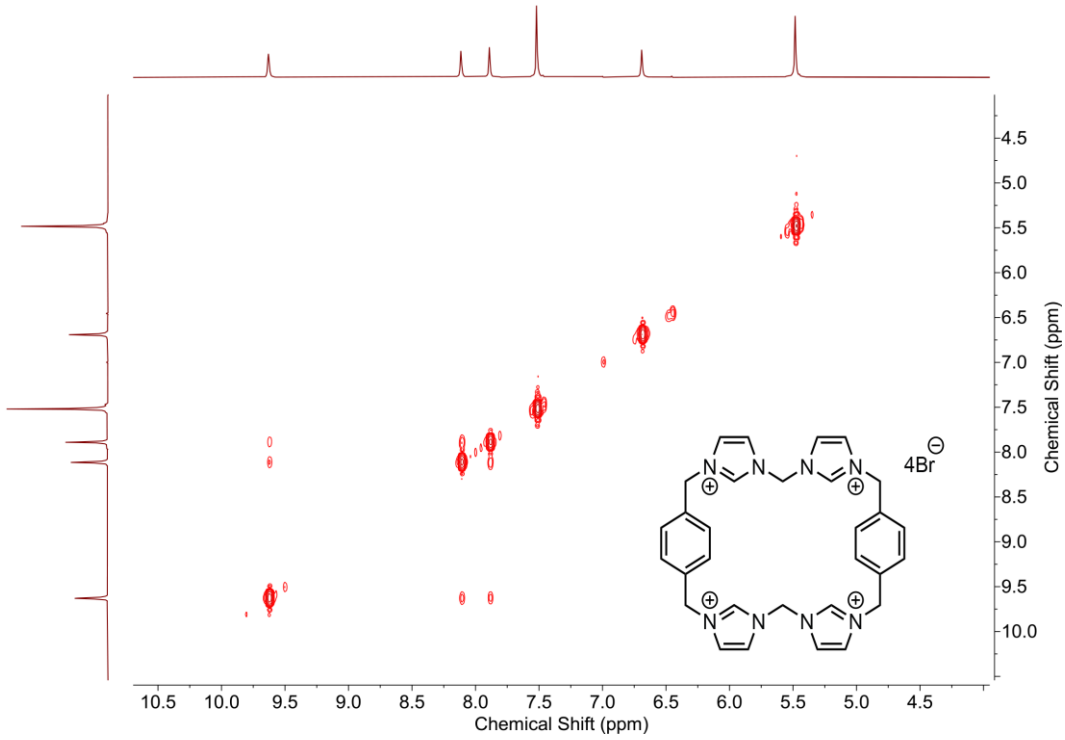

Figure S-8. ^1H COSY NMR spectrum of **PTI•Br** (DMSO-d_6, 600 MHz, 298K).

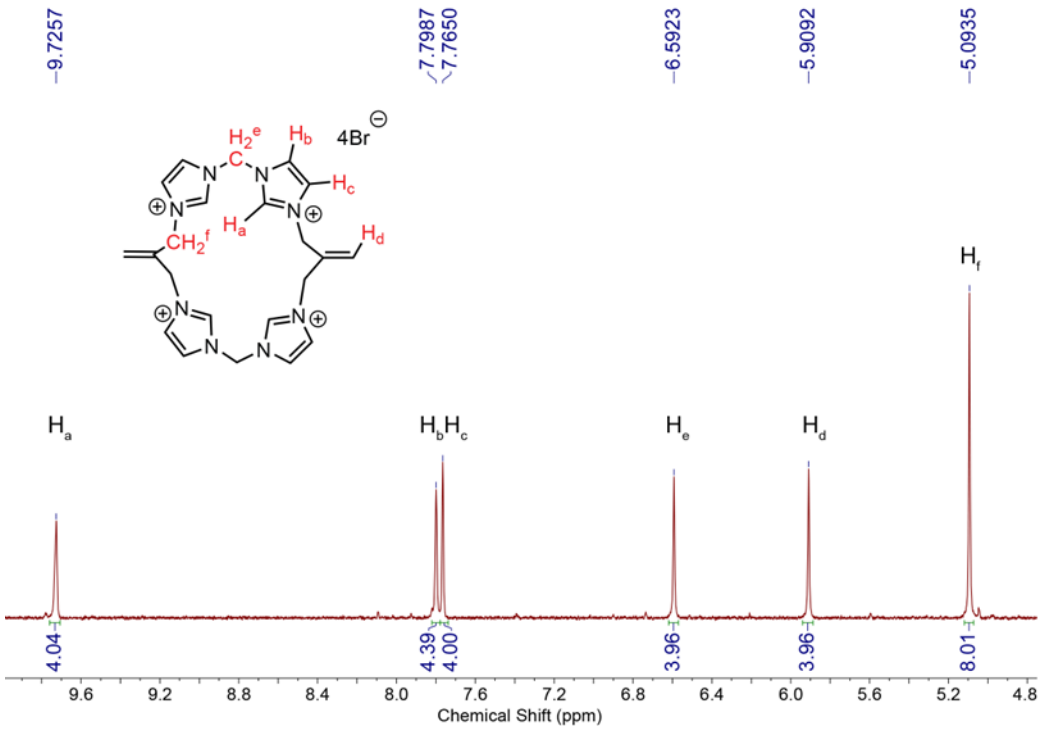

Figure S-9. ^{1}H NMR spectrum of **ATI•Br** (DMSO-d_6, 600 MHz, 298K).

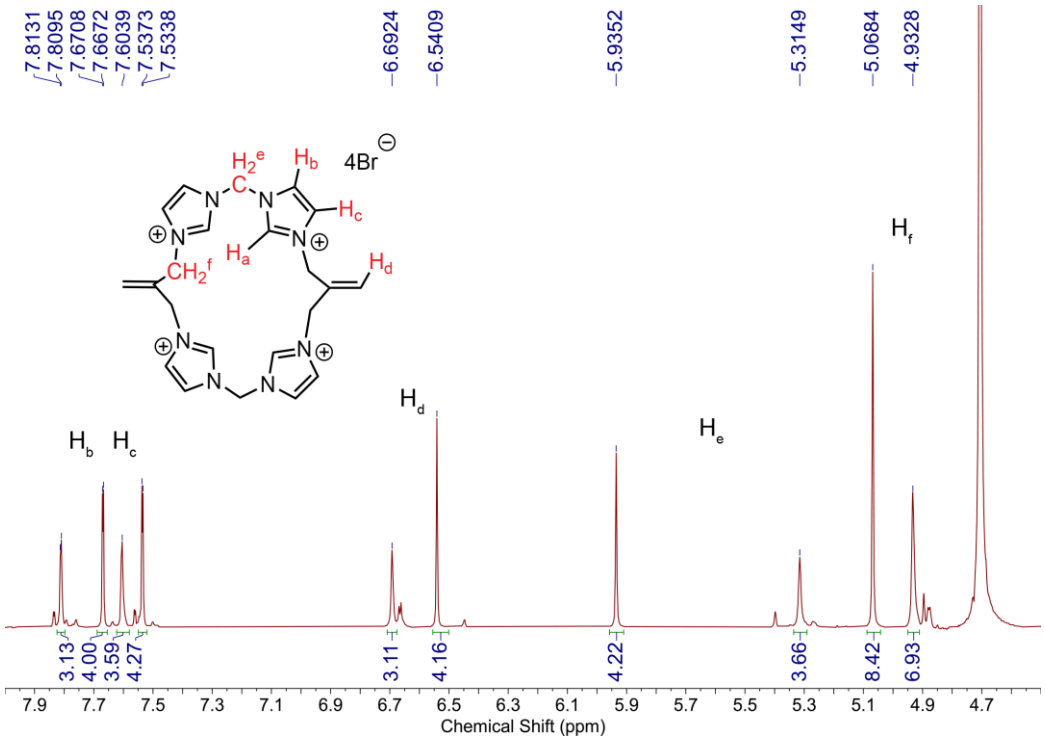

Figure S-10. ^{1}H NMR spectrum of **ATI•Br** (D_2O, 400 MHz, 298K).

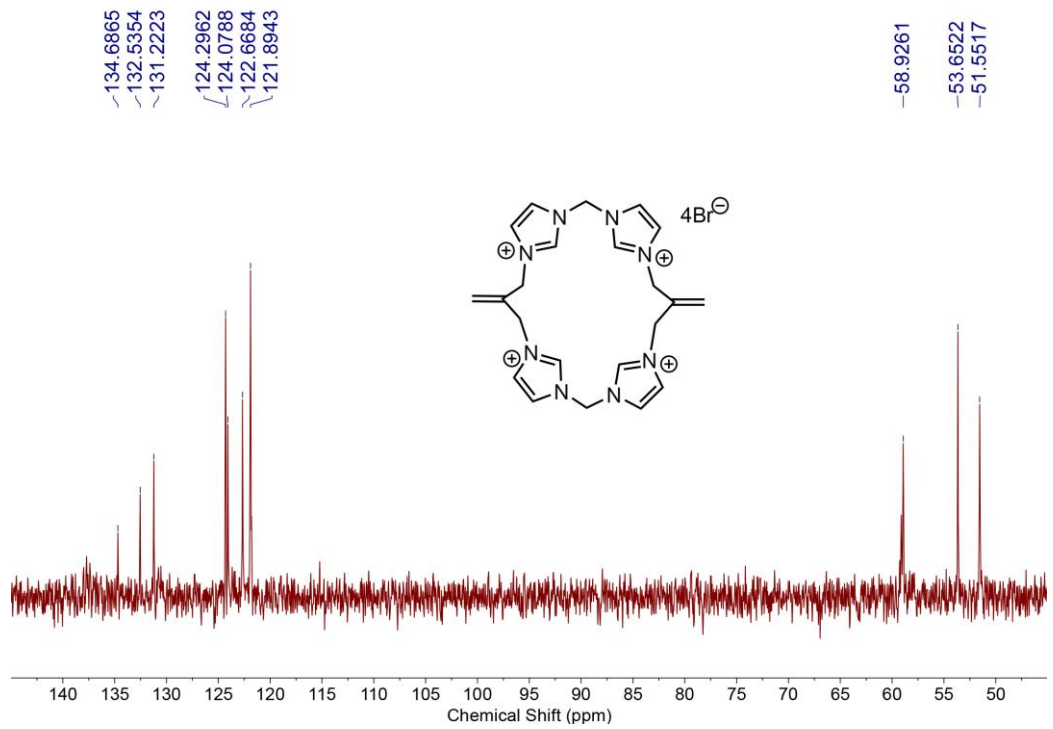

Figure S-11. $^{13}C\{^{1}H\}$ NMR spectrum of **ATI•Br** (D_2O, 101 MHz, 298K).

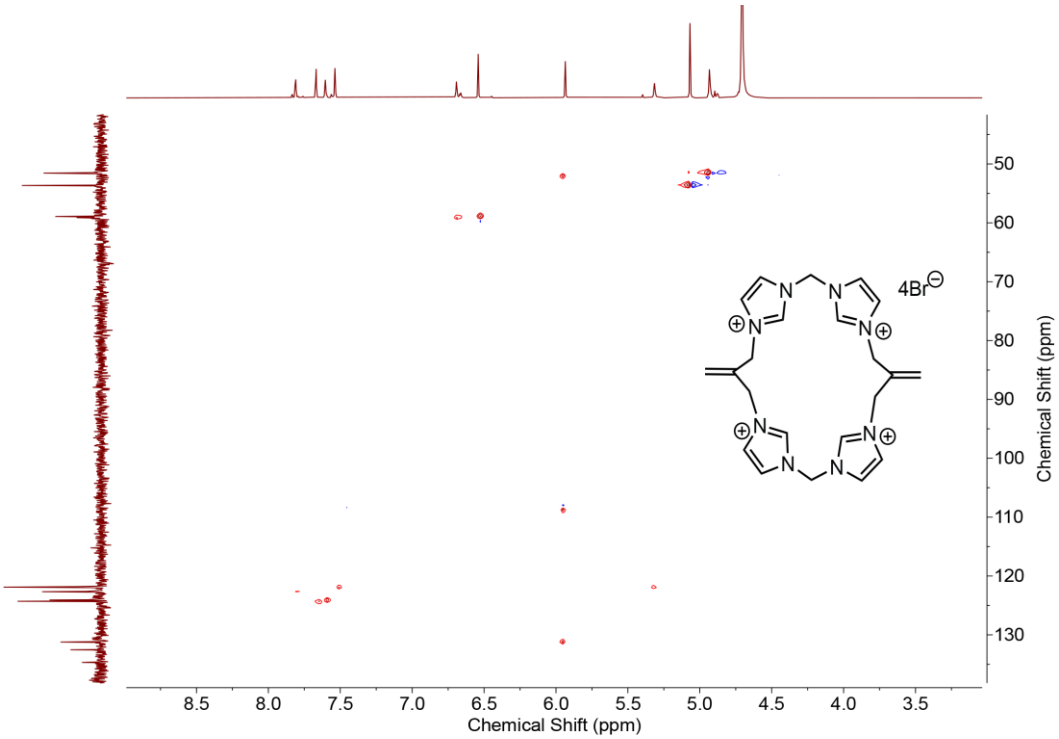

Figure S-12. HSQC NMR spectrum of **ATI•Br** (D_2O, 600 MHz, 298K).

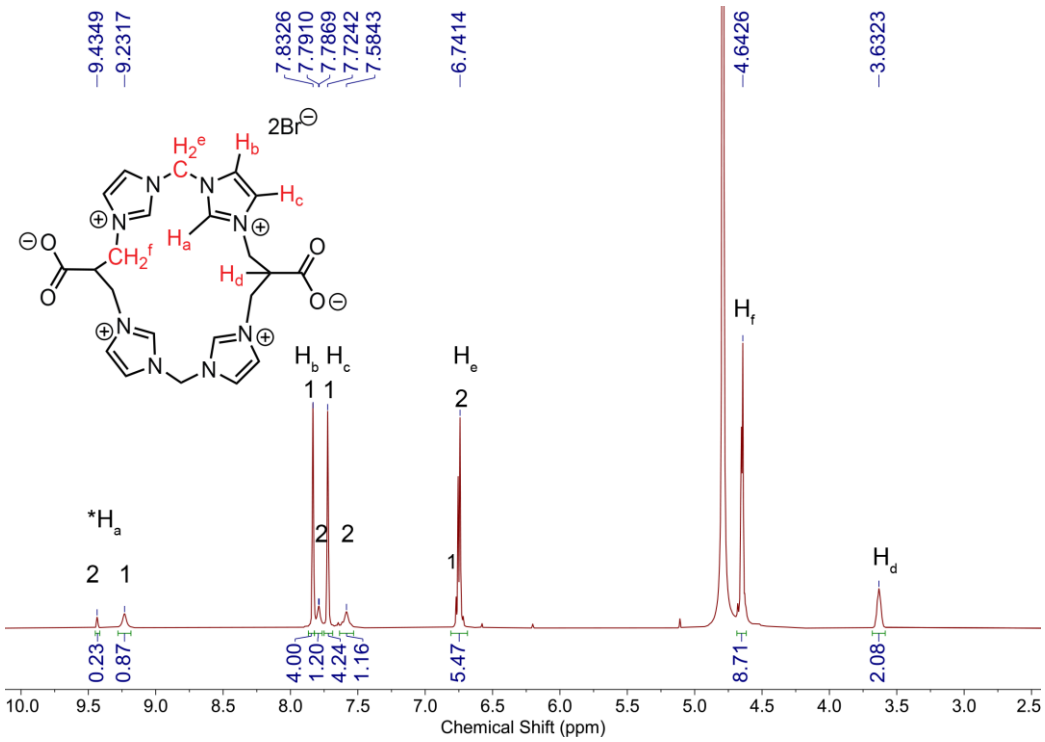

Figure S-13. ^{1}H NMR spectrum of **CTI•Br** (D_2O, 600 MHz, 298K). * Denotes proton that undergoes H-D exchange.

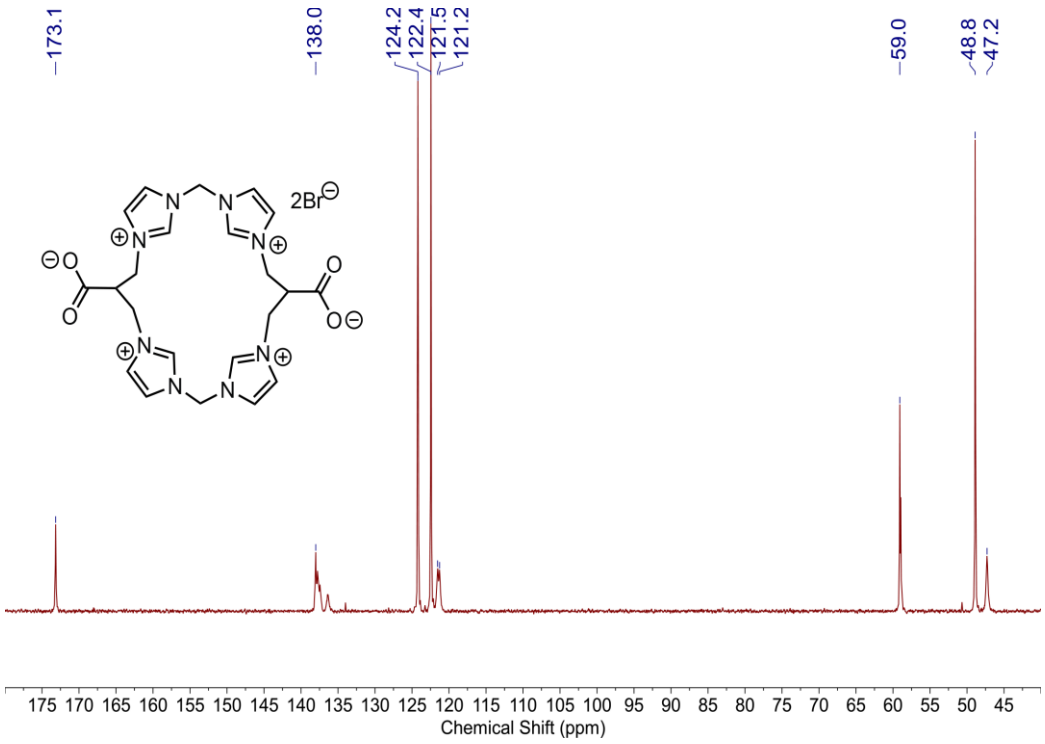

Figure S-14. ^{13}C{^{1}H} NMR spectrum of **CTI•Br** (D_2O, 101 MHz, 298K).

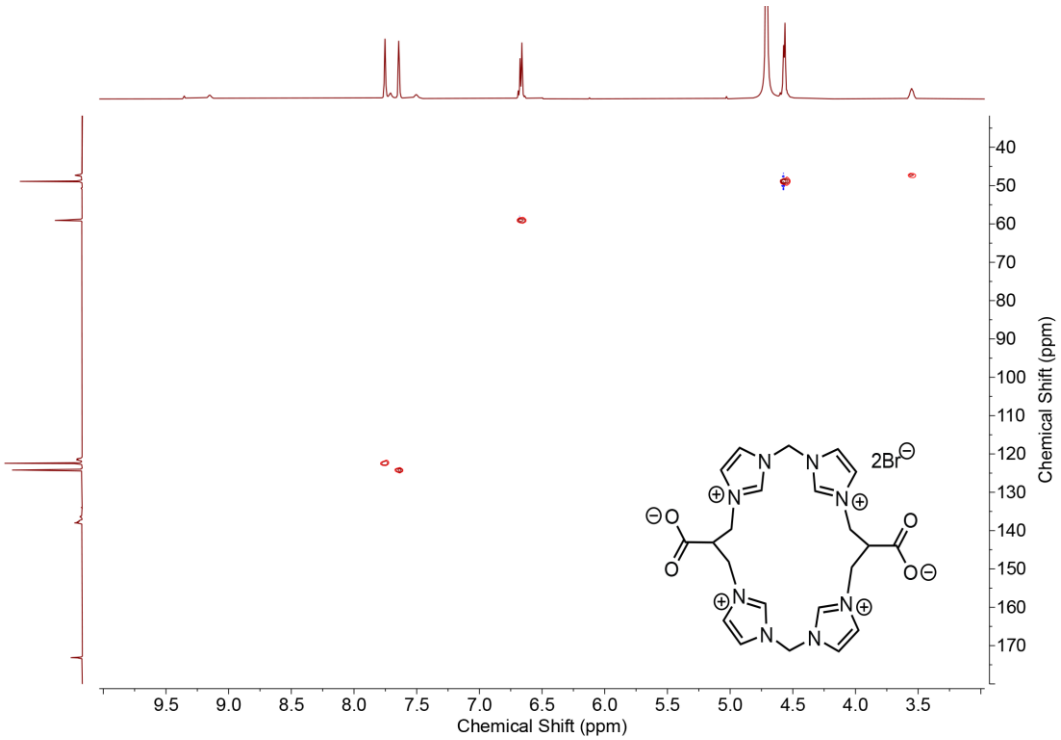

Figure S-15. HSQC NMR spectrum of **CTI•Br** (D_2O, 600 MHz, 298K).

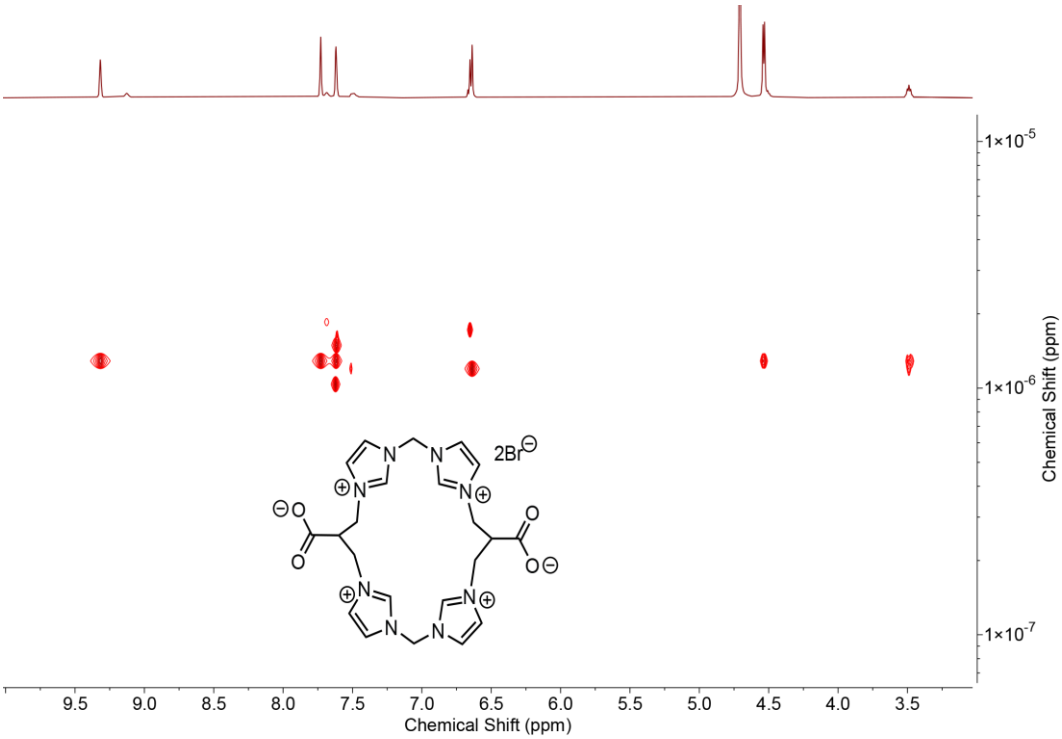

Figure S-16. DOSY NMR spectrum of **CTI•Br** (D_2O, 600 MHz, 298K) Diffusion constant 1.28 x 10^{-6} cm^2/sec and 1.73 x 10^{-6} cm^2/sec.

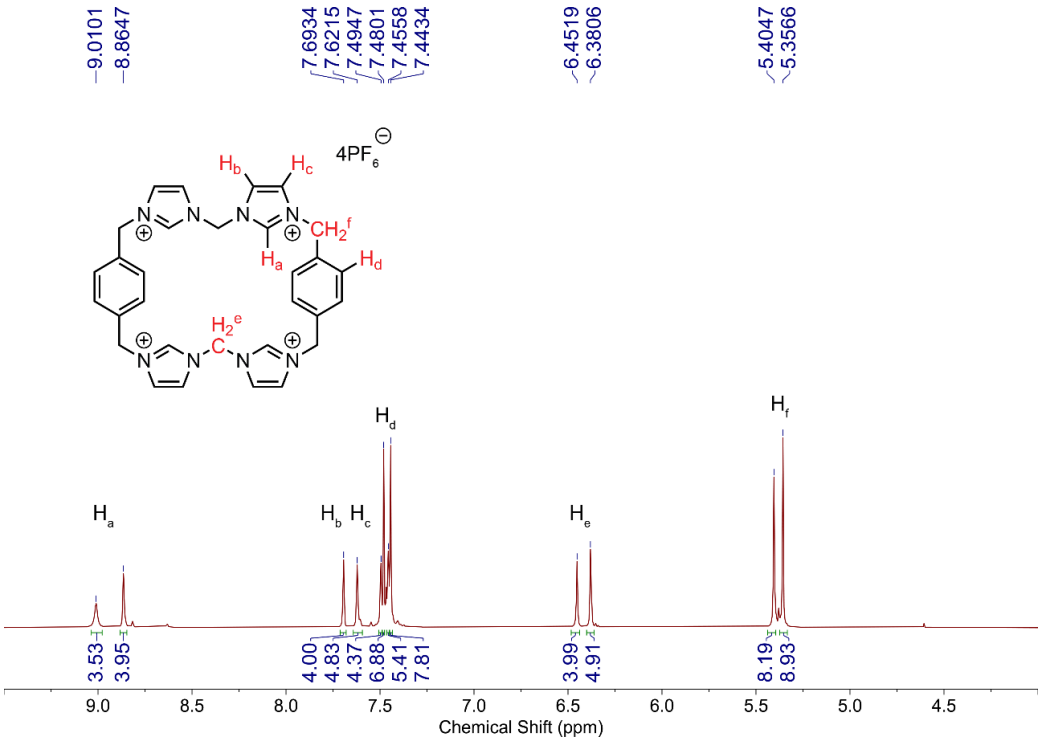

Figure S-17. ^{1}H NMR spectrum of **PTI•PF$_6$** (CD_3CN, 600 MHz, 298K).

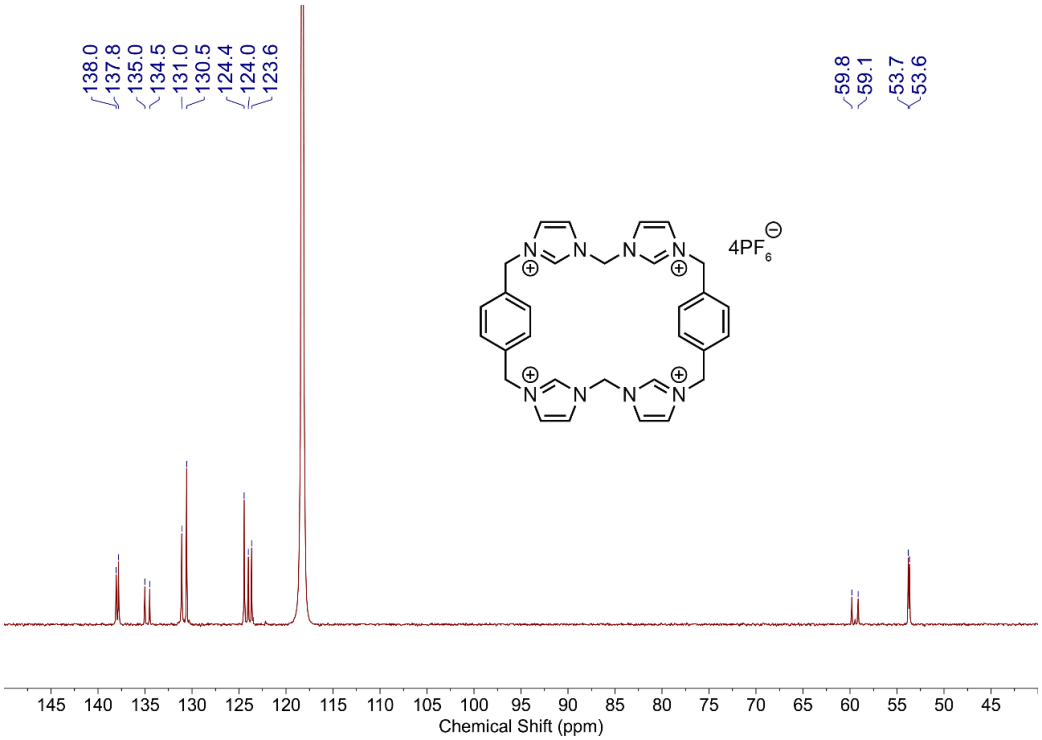

Figure S-18. ^{13}C{^{1}H} NMR spectrum of **PTI•PF$_6$** (CD_3CN, 101 MHz, 298K).

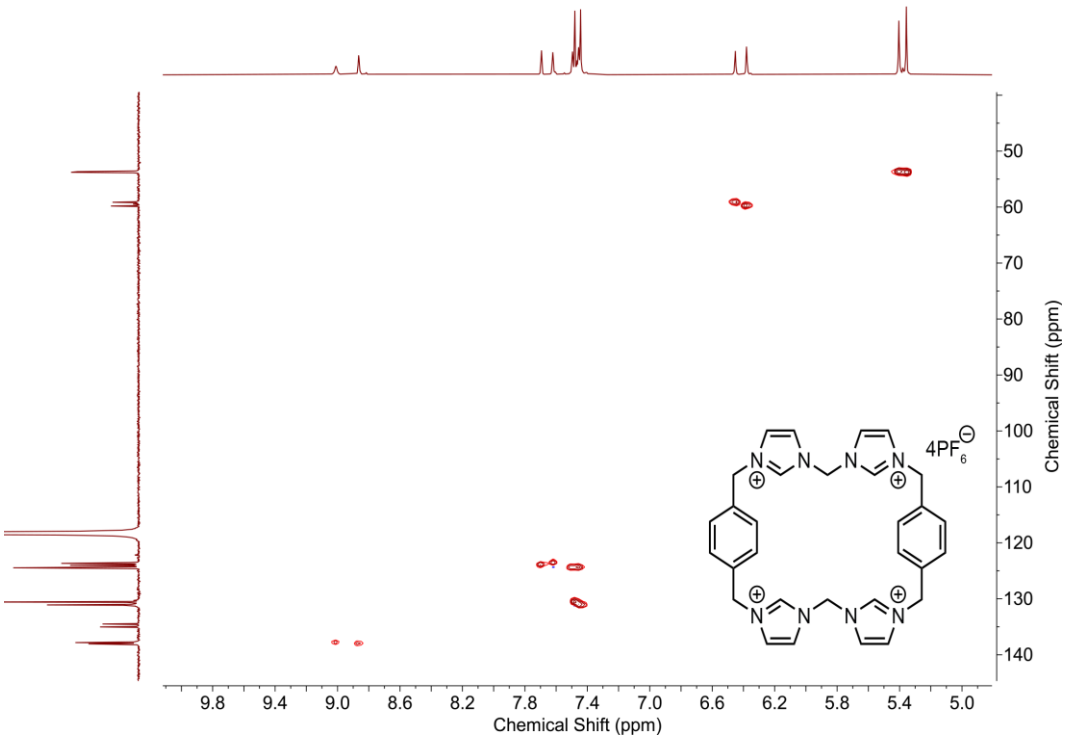

Figure S-19. HSQC NMR spectrum of **PTI•PF$_6$** (CD_3CN, 600 MHz, 298K).

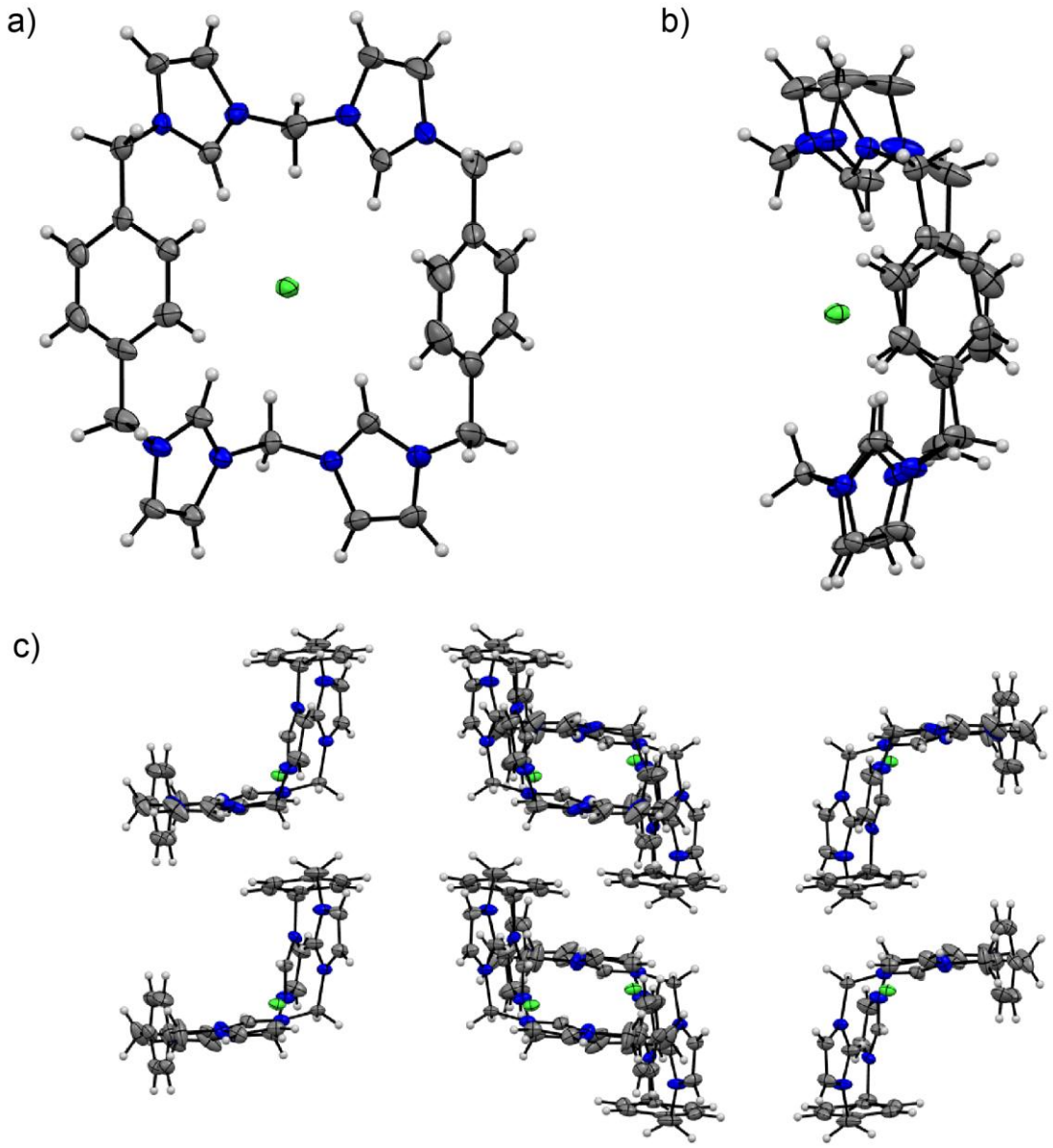

Figure S-20. Solid state structure of $[C_{30}H_{32}N_8Cl][PF_6]$ a) front view b) side view c) Packing unit. Grey, blue, green, and white ellipsoids represent carbon, nitrogen, chloride, and hydrogen. Ellipsoids are shown at 50% probability levels. Solvent (CHC_3N) and counter anions (PF_6) are removed for clarity.

2.2 NMR Titration

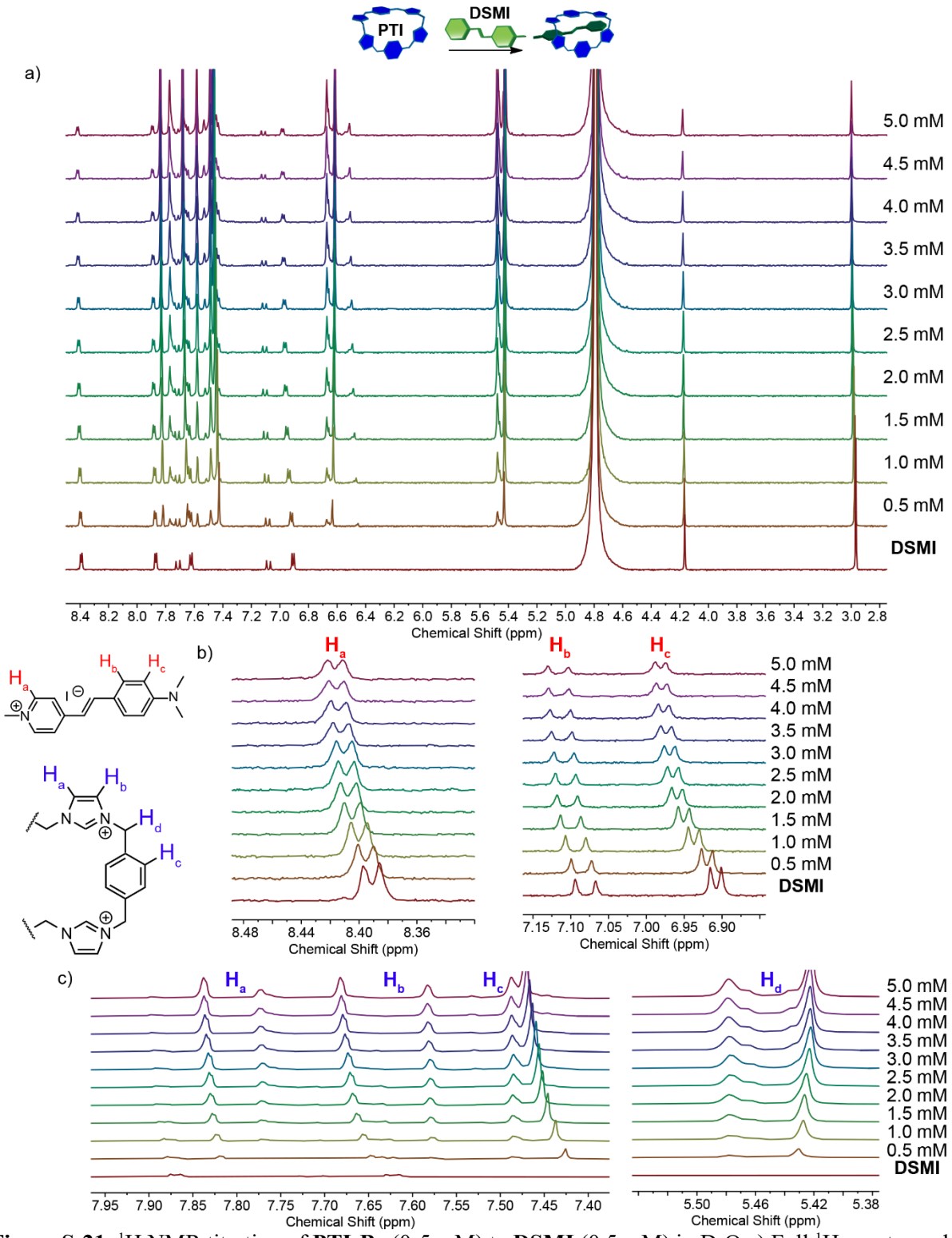

Figure S-21. ^{1}H NMR titration of **PTI•Br** (0-5 mM) to **DSMI** (0.5 mM) in D_2O a) Full ^{1}H spectrum: b) **DSMI** peak shifts: c) **PTI•Br** peak shifts.

3. Fluorescence Titrations

3.1 XTI-Dye Titrations

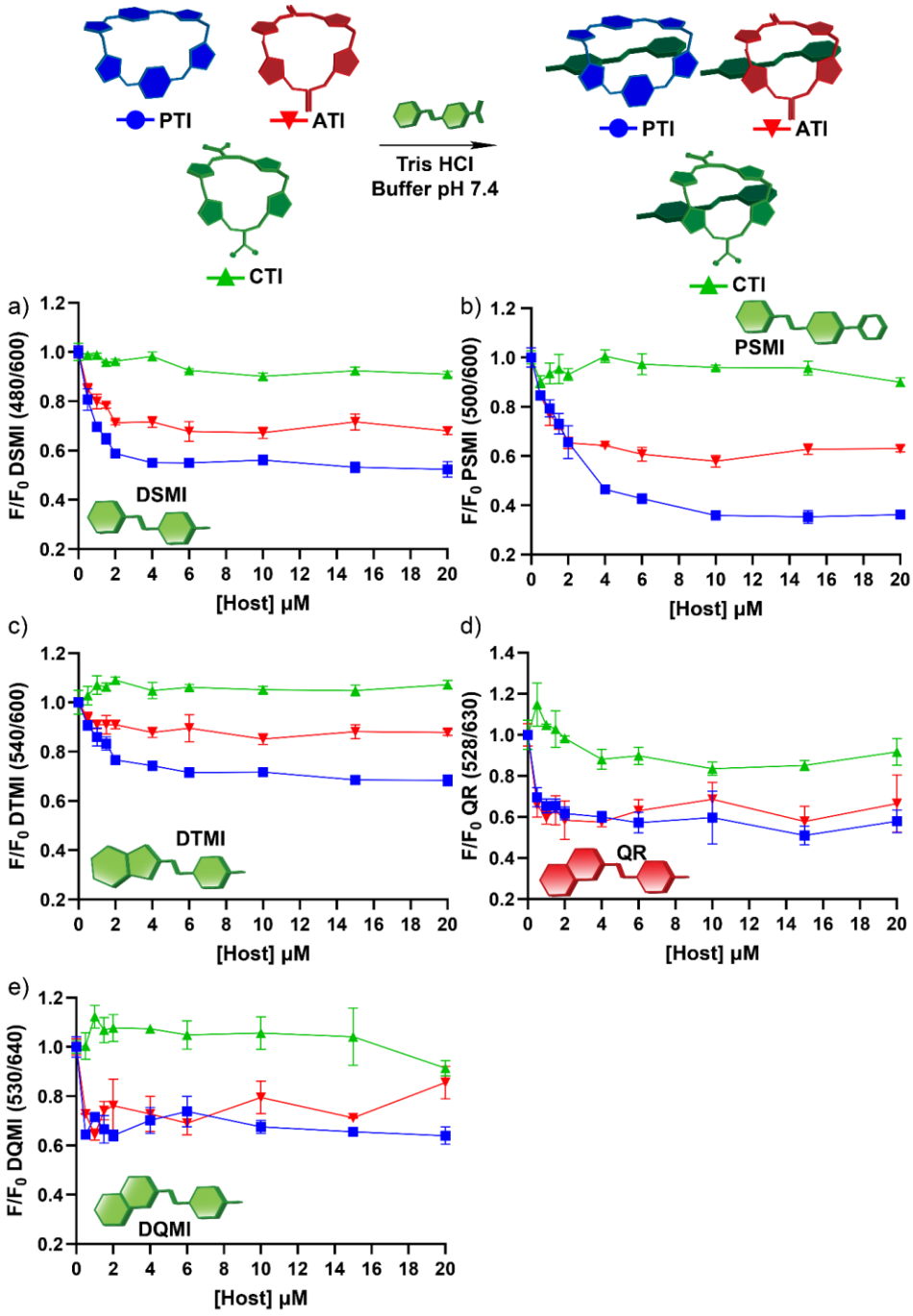

Figure S-22. Normalized fluorescence emission (F/F_0) titration curves of 0.5 µM dye and increasing concentration of **XTI** (**PTI•Br**, **ATI•Br**, **CTI•Br**) 0-20 µM in 20 mM Tris-HCl buffer at pH 7.4: a) **DSMI•XTI**; b) **PSMI•XTI**; c) **DTMI•XTI**; d) **QR•XTI**; e) **DQMI•XTI**.

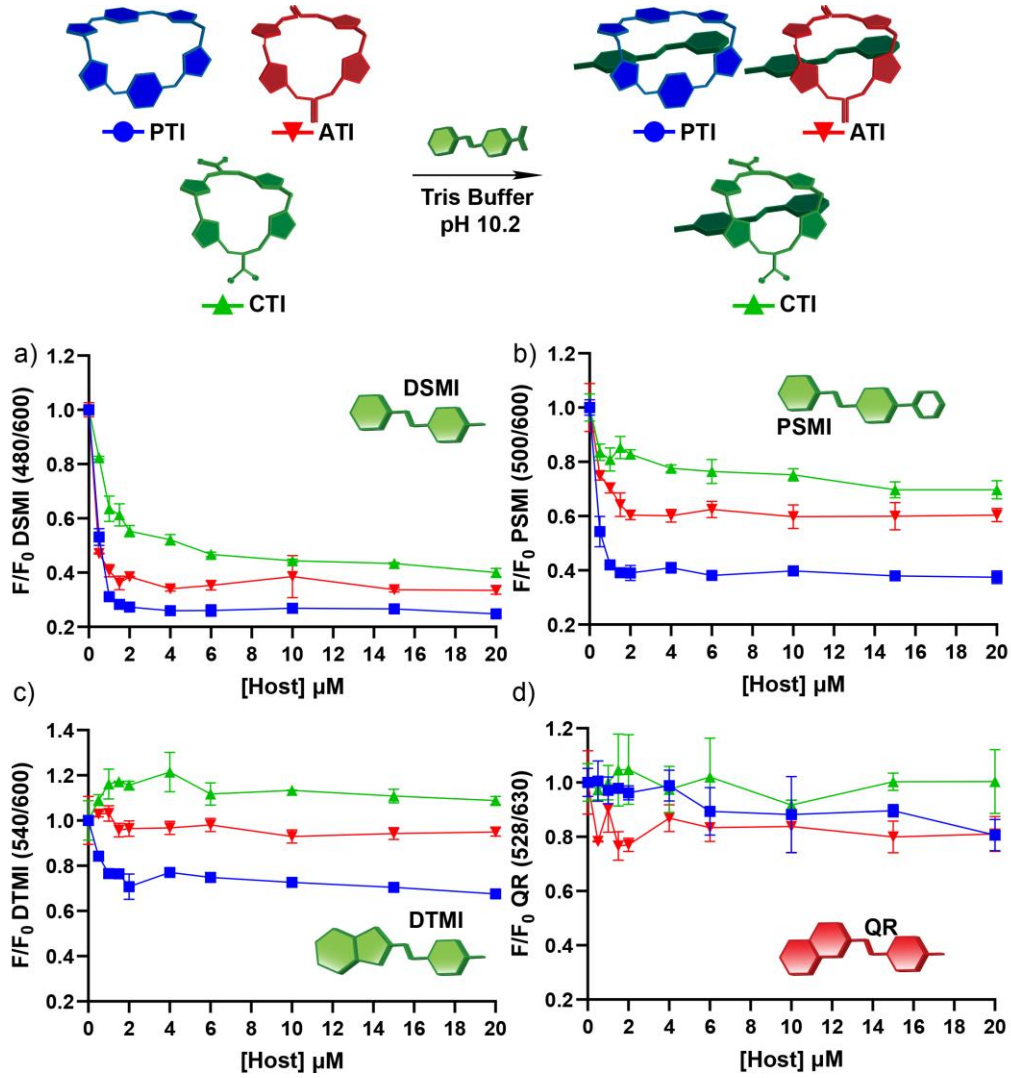

Figure S-23. Normalized fluorescence emission (F/F_0) titration curves of 0.5 µM dye and increasing concentration of **XTI** (**PTI•Br**, **ATI•Br**, **CTI•Br**) 0-20 µM in 20 mM Tris-HCl buffer at pH 10.2: a) **DSMI•XTI**; b) **PSMI•XTI**; c) **DTMI•XTI**; d) **QR•XTI**.

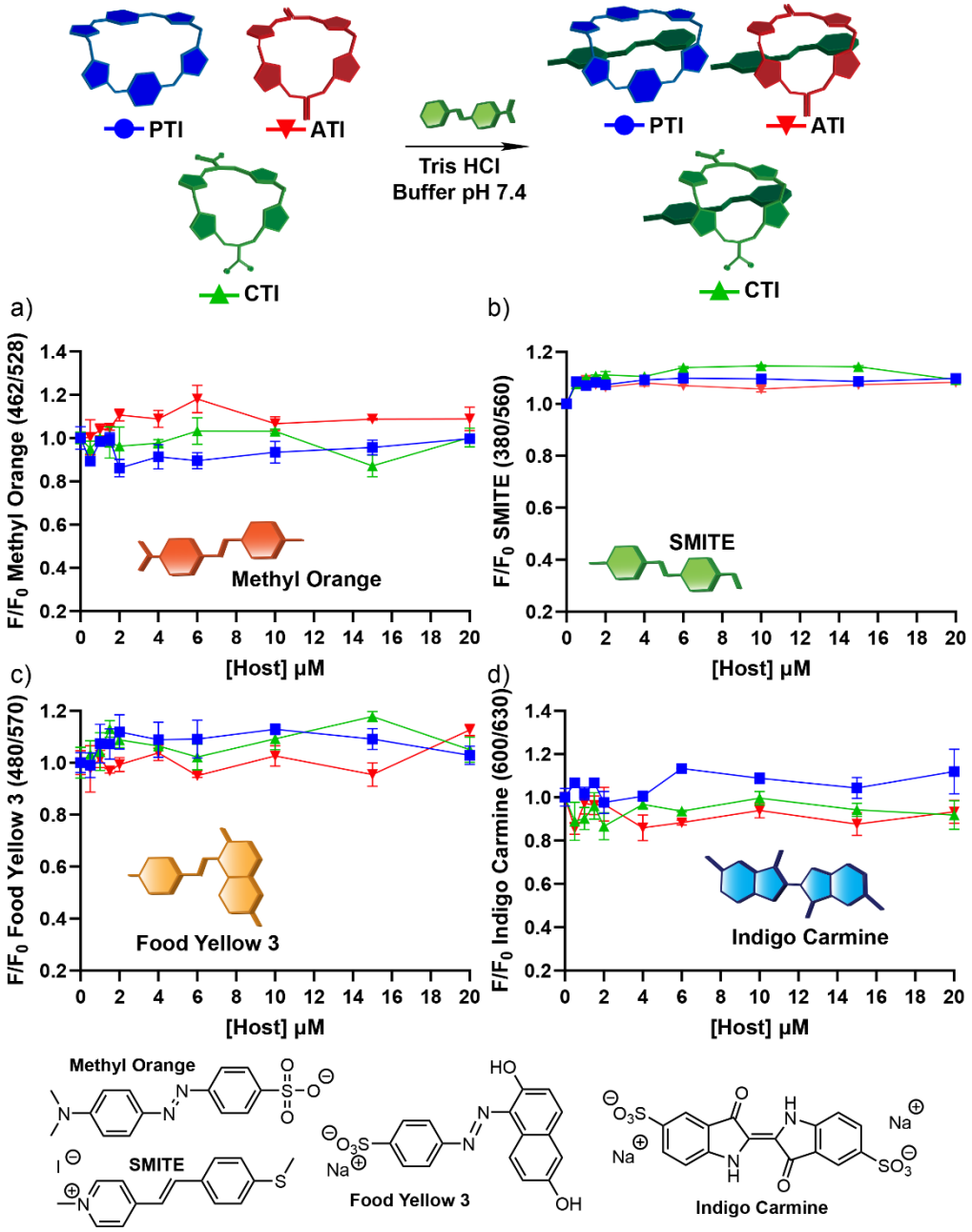

Figure S-24. Normalized fluorescence emission (F/F_0) titration curves of 0.5 µM dye and increasing concentrations of **XTI** (**PTI•Br**, **ATI•Br**, **CTI•Br**) 0-20 µM in 20 mM Tris-HCl buffer at pH 7.4: a) **Methyl Orange•XTI**; b) **SMITE•XTI**; c) **Food Yellow 3•XTI**; d) **Indigo Carmine•XTI**.

3.2 XTI:Dye Affinity in Tris-HCl Buffer

Table S-2. Measured K_d of **XTI** (**PTI•Br**, **ATI•Br**, **CTI•Br**) and dyes (**DSMI**, **DTMI**, **PSMI**, **QR, DQMI**) in Tris-HCl Buffer pH 7.4 & Tris Buffer pH=10.2.

	Tris Buffer-HCl pH 7.4			Tris Buffer pH 10.2		
K_d ± error (μM)	**PTI•Br**	**ATI•Br**	**CTI•Br**	**PTI•Br**	**ATI•Br**	**CTI•Br**
DSMI	0.4 ± 0.07	0.5 ± 0.2	9.7 ± 6.8	0.09 ± 0.07	0.08 ± 0.06	0.6 ± 0.2
DTMI	1.0 ± 0.2	0.9 ± 0.8	No binding	4.2 ± 4.1	No binding	No binding
PSMI	1.9 ± 0.4	0.5 ± 0.2	No binding	0.05 ± 0.02	0.2 ± 0.08	2.8 ± 2.3
QR	0.8 ± 0.7	No binding	No binding	45 ± 17	Failed	No binding

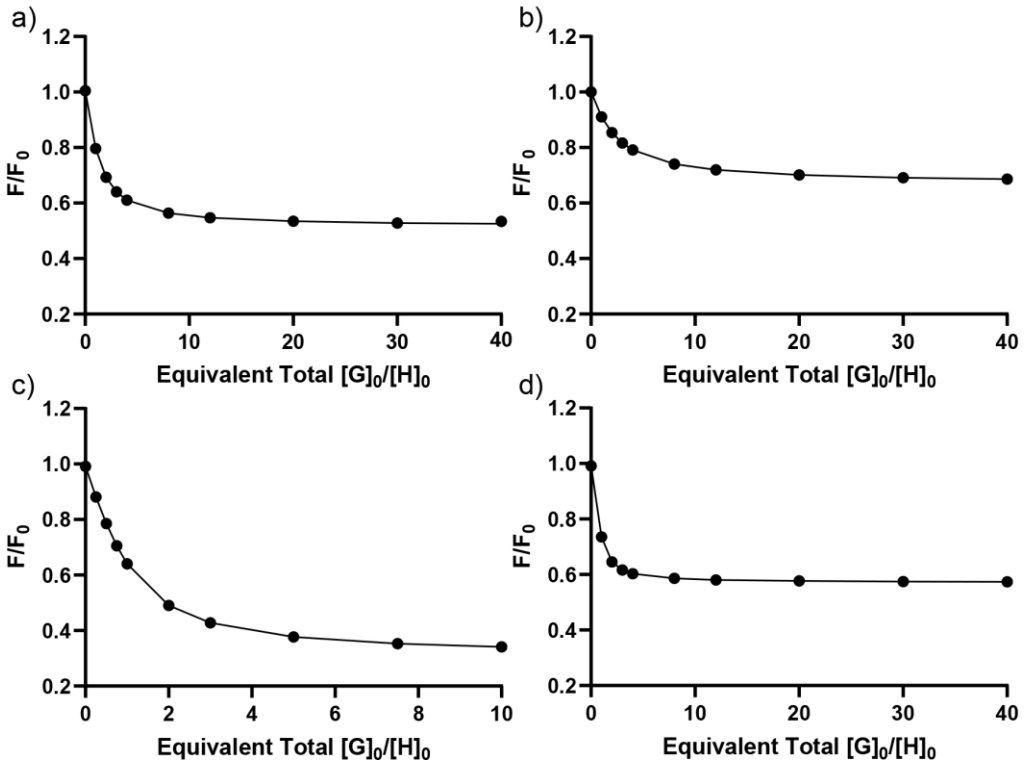

Figure S-25. Bindfit plot for dye: PTI•Br interaction in 20 mM Tris-HCl buffer pH 7.4: a) **DSMI**; b) **DTMI**; c) **PSMI**; d) **QR**.

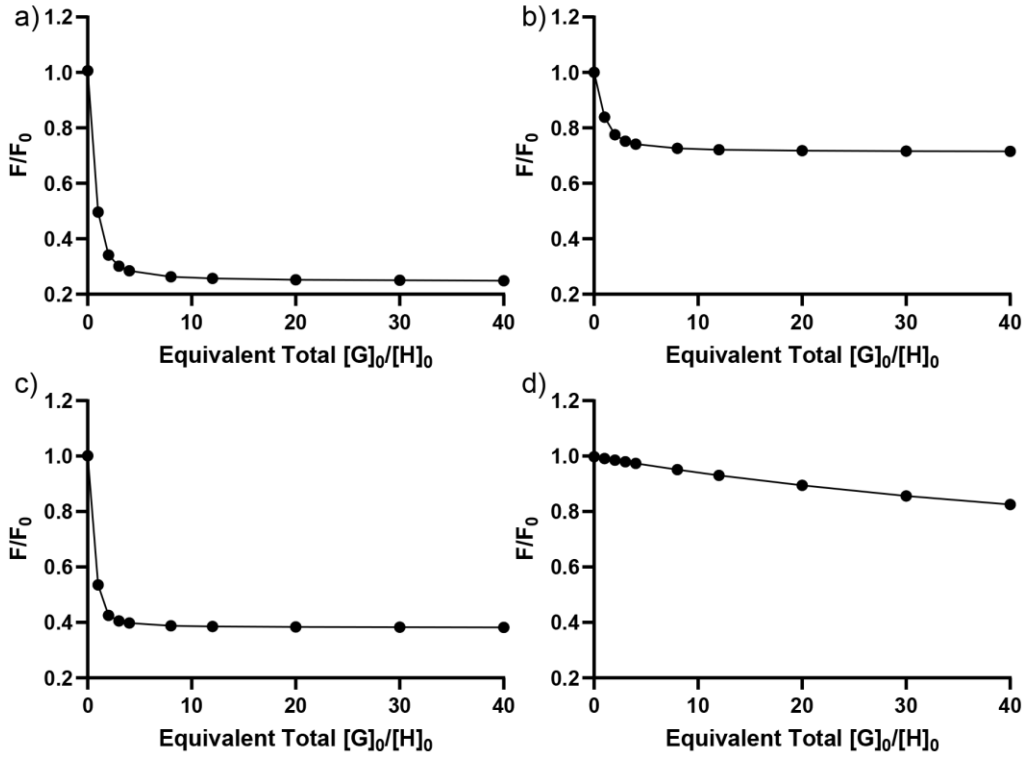

Figure S-26. Bindfit plot for dye: PTI•Br interaction in 20 mM Tris-HCl buffer pH 10.2: a) **DSMI**; b) **DTMI**; c) **PSMI**; d) **QR**.

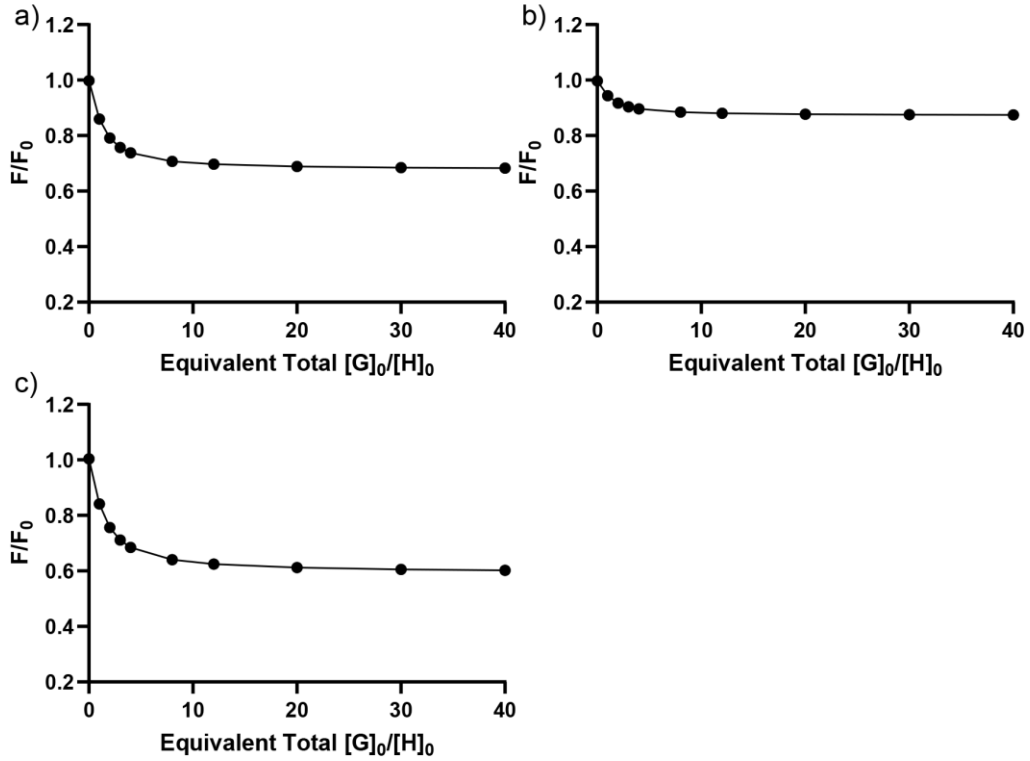

Figure S-27. Bindfit plot for dye: **ATI•Br** interaction in 20 mM Tris-HCl buffer pH 7.4: a) **DSMI**; b) **DTMI**; c) **PSMI**.

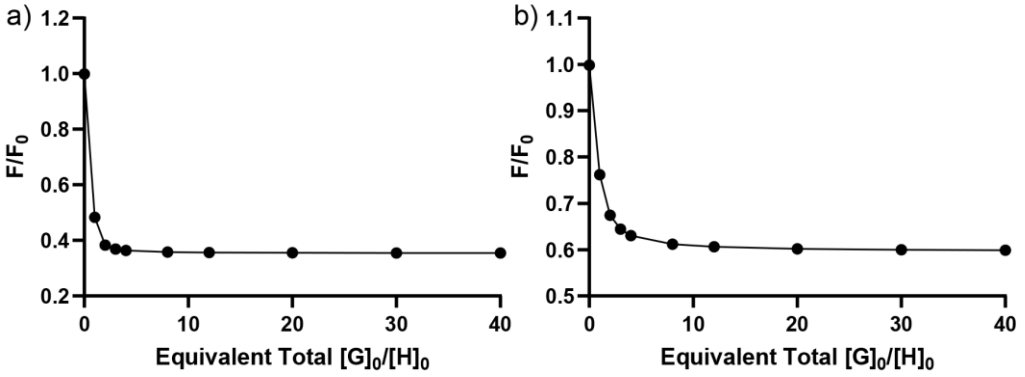

Figure S-28. Bindfit plot for dye: **ATI•Br** interaction in 20 mM Tris-HCl buffer pH 10.2: a) **DSMI**; b) **PSMI**.

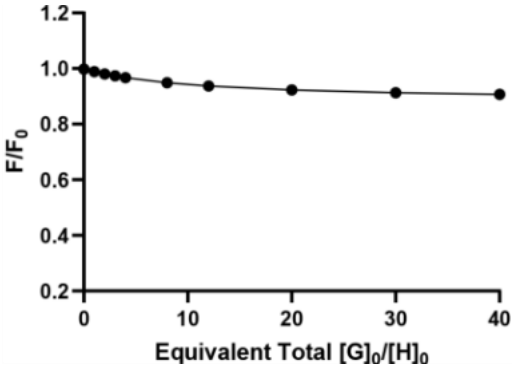

Figure S-29. Bindfit plot for dye: **CTI•Br** interaction in 20 mM Tris-HCl buffer pH 7.4: **DSMI**

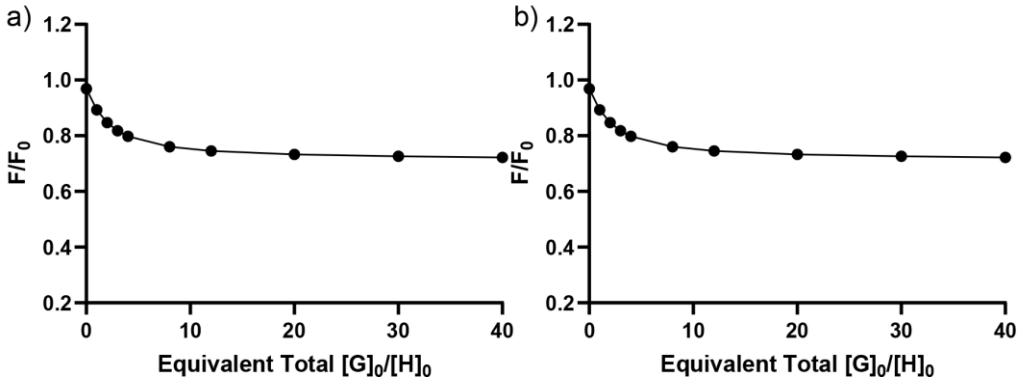

Figure S-30. Bindfit plot for dye**: CTI•Br** interaction in 20 mM Tris buffer pH 10.2: a) **DSMI**; b) **PSMI**.

3.3 Salt Effect on DSMI and PTI Binding

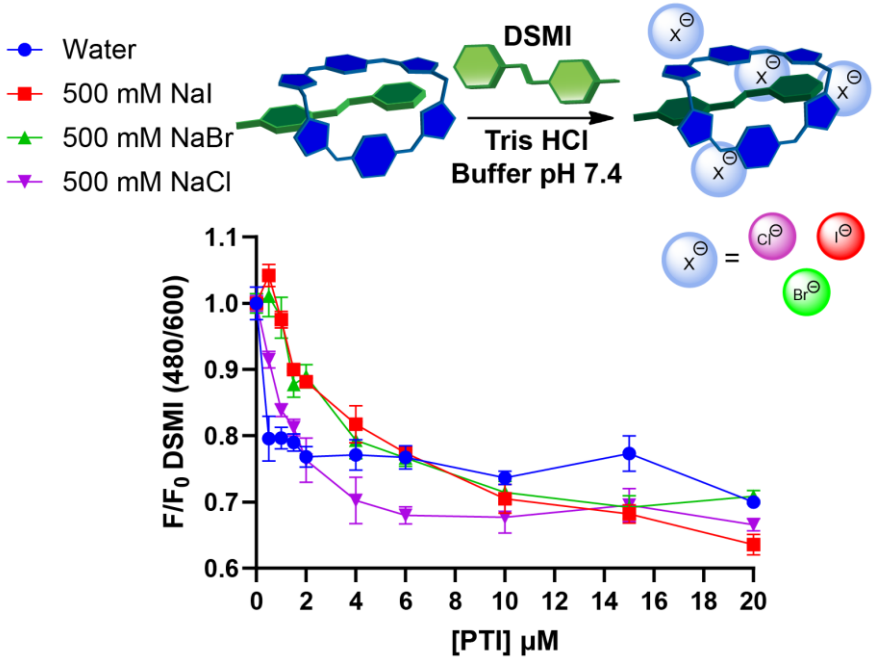

Figure S-31. Normalized fluorescence emission (F/F_0) of 0-20 µM **PTI•Br** and 0.5 µM **DSMI** in the presence of 500 mM salt (NaI, NaBr, NaCl) in water.

Table S-3. Measured K_d of **PTI** and **DSMI** in the presence of 500 mM salt (NaI, NaBr, and NaCl) in water.

K_d ± error (µM)	**PTI•Br**
Water	Failed
NaCl	0.9 ± 0.2
NaBr	3.3 ± 1.1
NaI	5.1 ± 1.3

3.4. Peptide Sequences Wdfy3 and Ptpn13

Table S-4 Peptide sequences applied in this study and properties of the wild-type (WT) Wdfy3 and Ptpn13 peptides. S* indicates a phosphorylated serine

No	Name	Sequence	a.a.	pI[a]	Net pH 7.4	GRAVY	Hydrophobicity [b]	M.W.[a]
1	Wdfy3 (WT)	DDSRRWSDQLSLD	13	3.87		-1.71	25.19	1592.85
2	WdfySp3	DDS*RRWSDQLSLD	13					1672.40
3	Wdfy3Sp7	DDSRRWSDQLS*LD	13					1672.40
4	Wdfy3Sp3Sp7	DDS*RRWSDQLS*LD	13					1752.60
5	Ptpn13 (WT)	EILKRLSSSEWSL	13	7	0.0	-0.28	34.49	1547.74
6	Ptpn13Sp7	EILKRLS*SSEWSL	13					1626.72

[a] Theoretical isoelectric point (pI), molecular weight (M.W.), net charge under pH 7.4 or pH 5, and grand average of hydropathicity (GRAVY)[22] of peptides were calculated using Peptide Property Calculator on NovoPro website (https://www.novoprolabs.com/tools/calc_peptide_property).

[b] The hydrophobicity of peptides was obtained using Peptide Synthesis and Proteotypic Peptide Analyzing Tool on Thermo Fisher Scientific website (https://www.thermofisher.com/us/en/home/life-science/protein-biology/peptides-proteins/custom-peptide-synthesis-services/peptide-analyzing-tool.html), which is based on the 'Oleg V. Krokhin' Index and takes into account difficult combinations, such as avoiding too many of the same amino acid in the row and too many hydrophobic amino acids.

3.5 XTI-Peptide Titrations

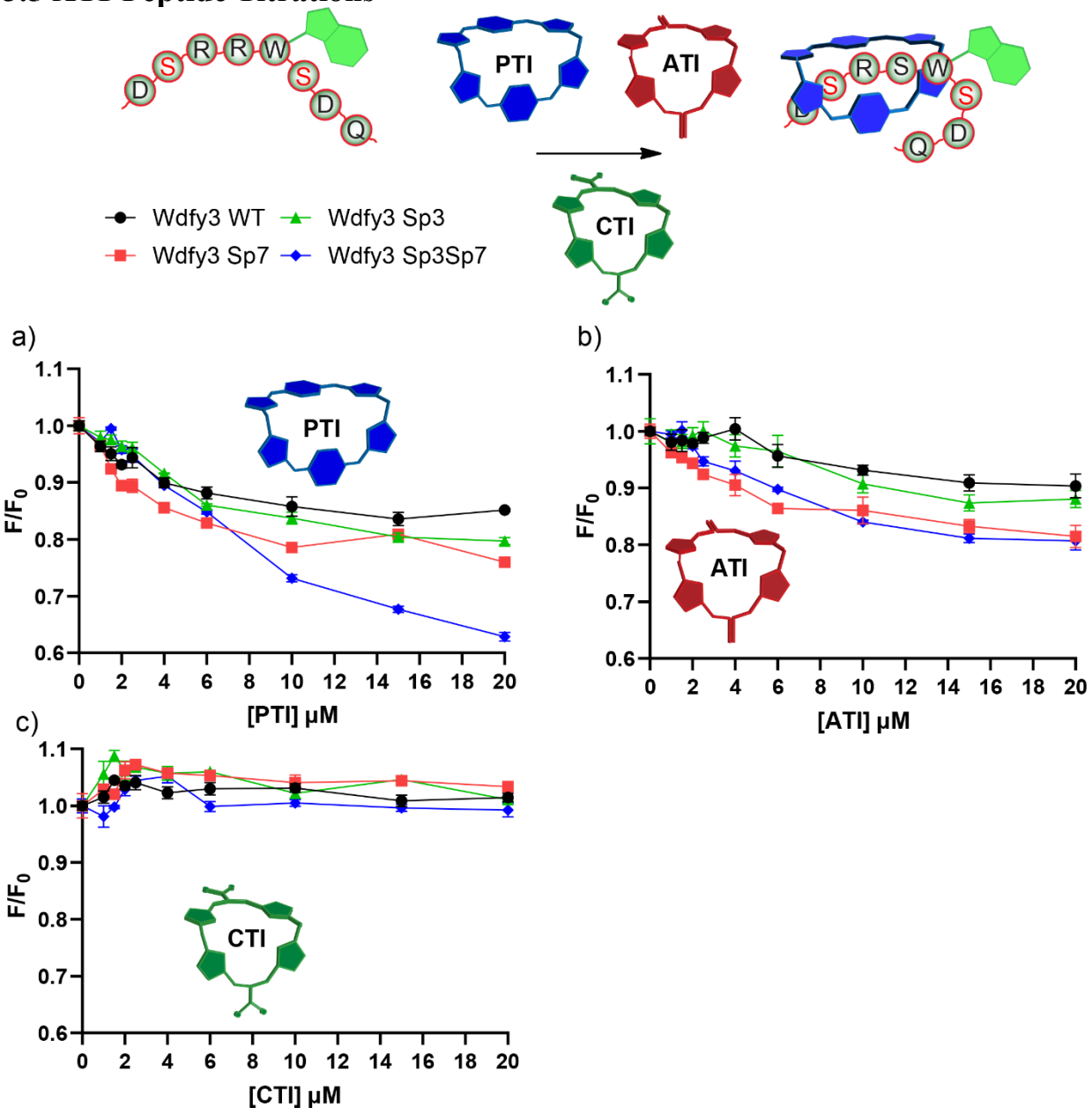

Figure S-32. Normalized fluorescence titration curves (F/F_0) of 2 µM Wdfy3 peptides (WT, Sp3, Sp7, and Sp3Sp7) monitored by the change in emission of Trp residues (Ex 280 nm/Em 354 nm) in 20 mM Tris-HCl at pH 7.4, upon addition of increasing concentrations (0-20 µM) of **XTI** (**PTI•Br**, **ATI•Br**, **CTI•Br**) compounds: a) **PTI•Br**; b) **ATI•Br**; c) **CTI•Br**.

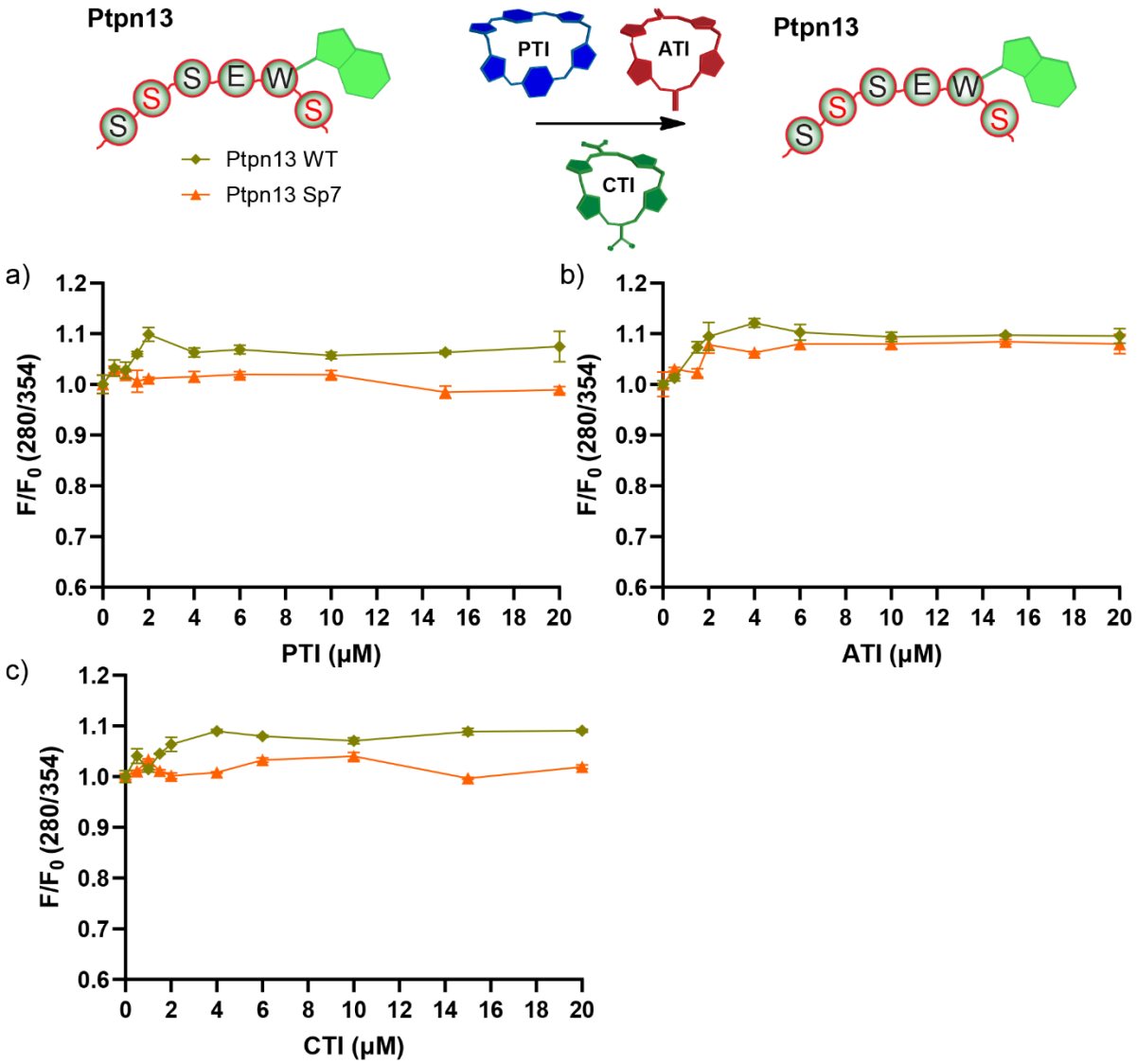

Figure S-33. Normalized fluorescence titration curves (F/F_0) of 2 μM Ptpn13 peptides (WT and Sp7) monitored by monitored by the change in emission of Trp residues (Ex 280 nm/Em 354 nm) in 20 mM Tris-HCl at pH 7.4, upon addition of increasing concentrations (0-20 μM) of **XTI** (**PTI•Br**, **ATI•Br**, **CTI•Br**) compounds: a) **PTI•Br**; b) **ATI•Br**; c) **CTI•Br**.

3.6 Dye:XTI— Peptide— Peptide Titrations

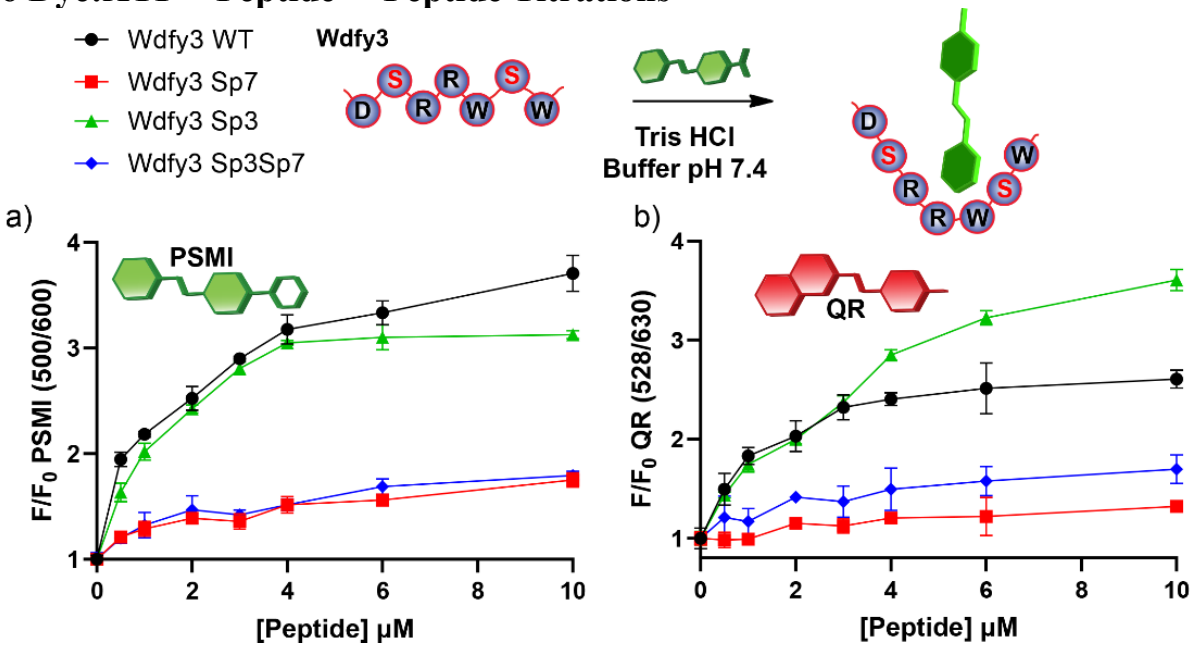

Figure S-34. Normalized fluorescence emission (F/F_0) titration curves of 0.5 µM dye (**PSMI, QR**) and increasing concentrations (0-20 µM) of Wdfy3 peptides (WT, Sp3, Sp7, and Sp3Sp7) in 20 mM Tris-HCl buffer at pH 7.4: a) **PSMI** and b) **QR**.

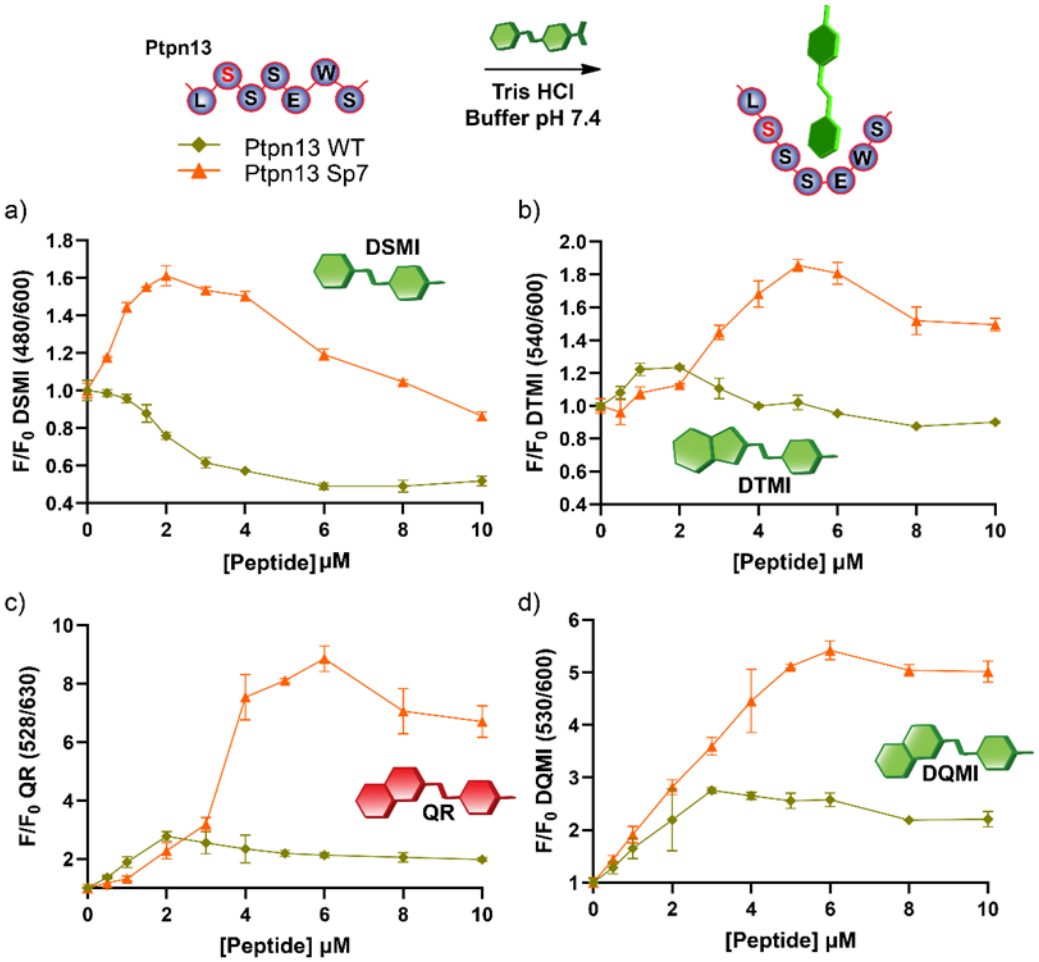

Figure S-35. Normalized fluorescence emission (F/F_0) titration curves of 0.5 µM dye and increasing concentrations (0–20 µM) of Ptpn13 peptides (WT and Sp7) in 20 mM Tris-HCl buffer at pH 7.4: a) **DSMI**; b) **DTMI**; c) **QR** and d) **DQMI**.

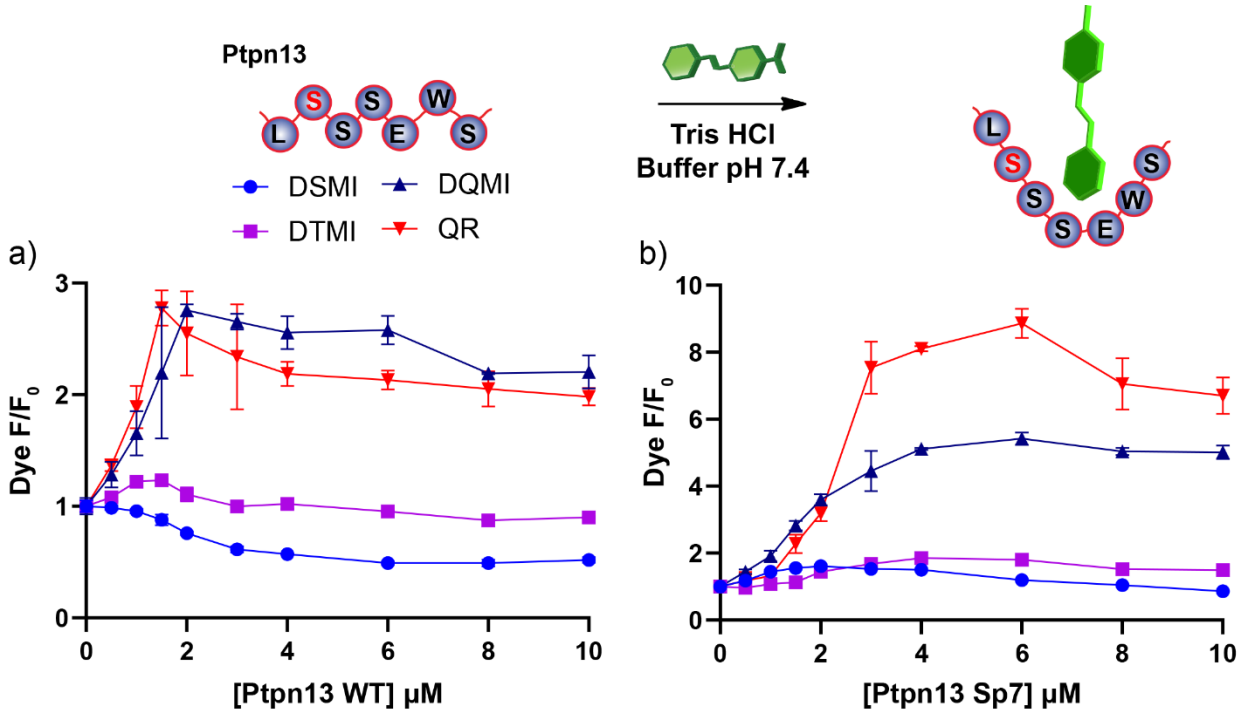

Figure S-36. Stacked normalized fluorescence emission (F/F_0) titration curves (Figure S-36) of 0.5 µM dye (**DSMI**, **DTMI**, **DQMI**, **QR**) and increasing concentration (0-20 µM) of Ptpn13 peptides (WT and Sp7) in 20 mM Tris-HCl buffer at pH 7.4: a) Ptpn13 WT and b) Ptpn13 Sp7.

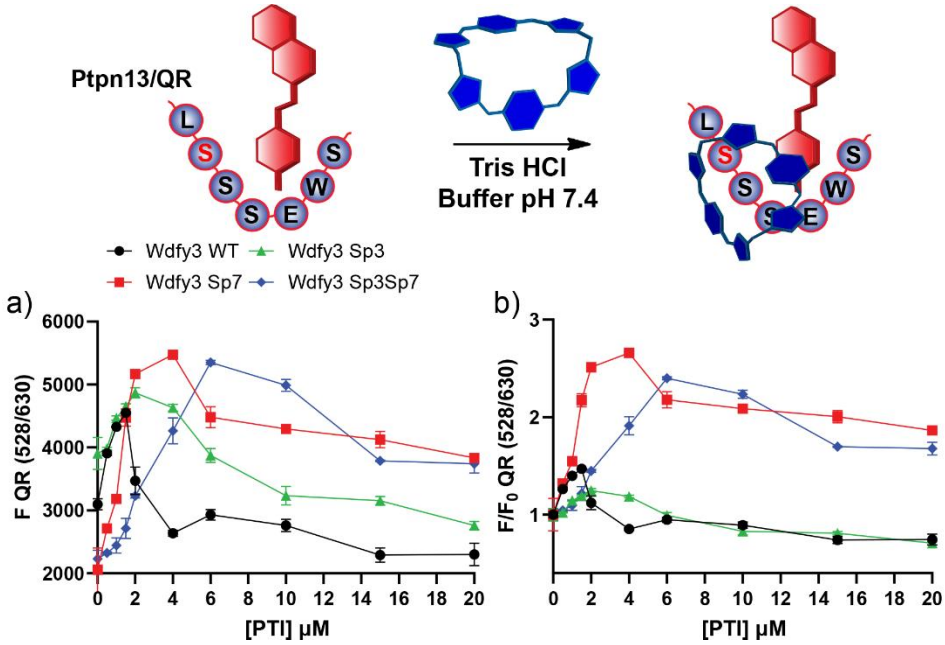

Figure S-37. Fluorescence emission titration curves of 0.5 µM **QR**, 4 µM of Wdfy3 peptides (WT**,** Sp7, Sp3, and Sp3Sp7) and increasing concentrations (0-20 µM) of **PTI•Br** in 20 mM Tris-HCl buffer at pH 7.4: a) F and b) F/F_0.

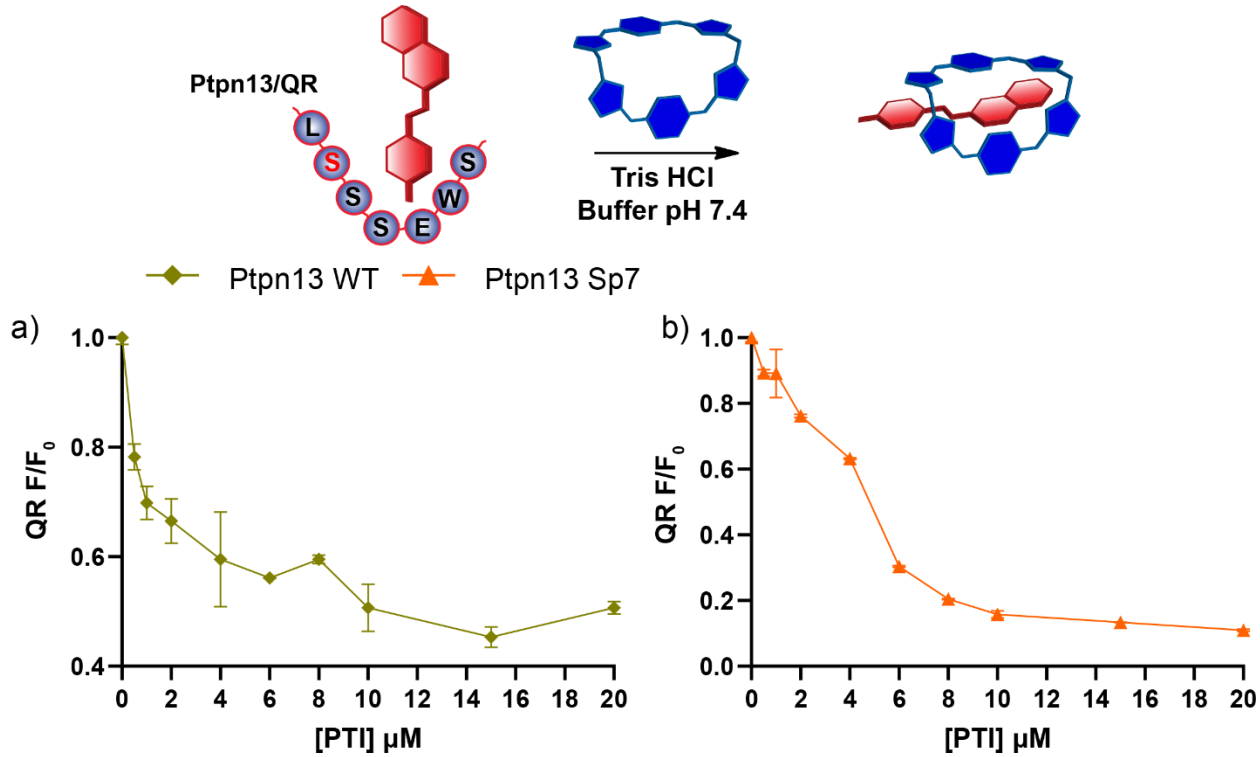

Figure S-38. Fluorescence emission titration curves of 0.5 µM **QR**, 4 µM of peptide (Ptpn13, Ptpn13Sp7) and increasing concentrations of **PTI•Br** (0-20 µM) in 20 mM Tris-HCl buffer in pH 7.4: a) F and b) F/F_0.

4. Molecular Dynamics Simulations

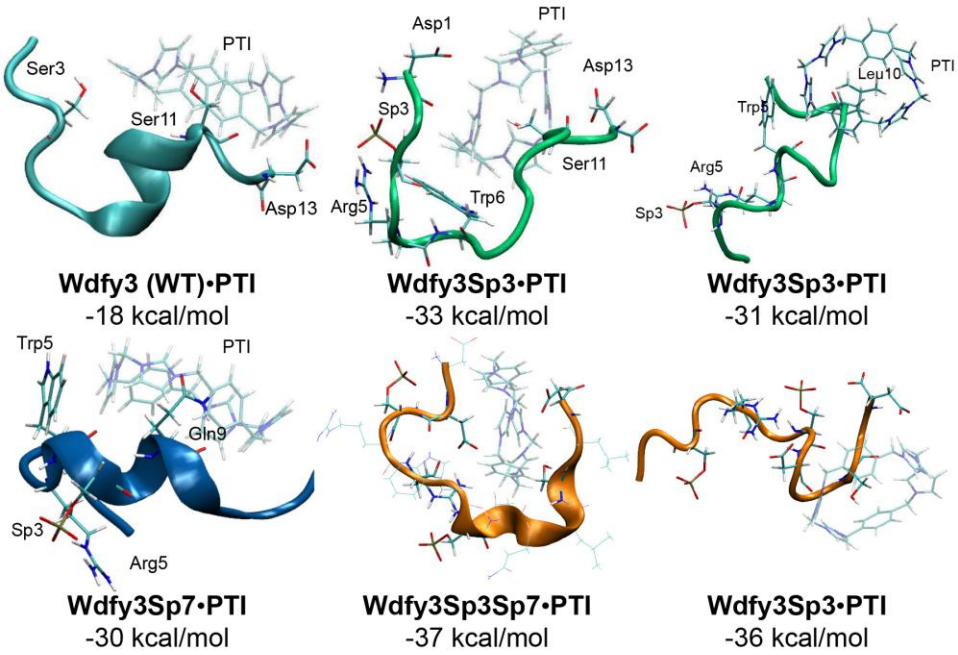

Figure S-39. Optimized conformations of peptides (Wdfy3 WT, Wdfy3 Sp3, Wdfy3 Sp7, and WdfySp3Sp7) with **PTI**.

Table S-5. Average interaction energy of peptides (kcal/mol) (**Wdfy3**, **Wdfy3Sp3**, **Wdfy3Sp7**, **Wdfy3Sp3Sp7**) with **PTI**

Peptide + PTI	Interaction energy (kcal/mol)
Wdfy3 WT	-4.7
Wdfy3 Sp3	-5.5
Wdfy3 Sp7	-7.5
Wdfy3 Sp3Sp7	-25.8

5. Array Sensing of Wdfy3 and Ptpn13

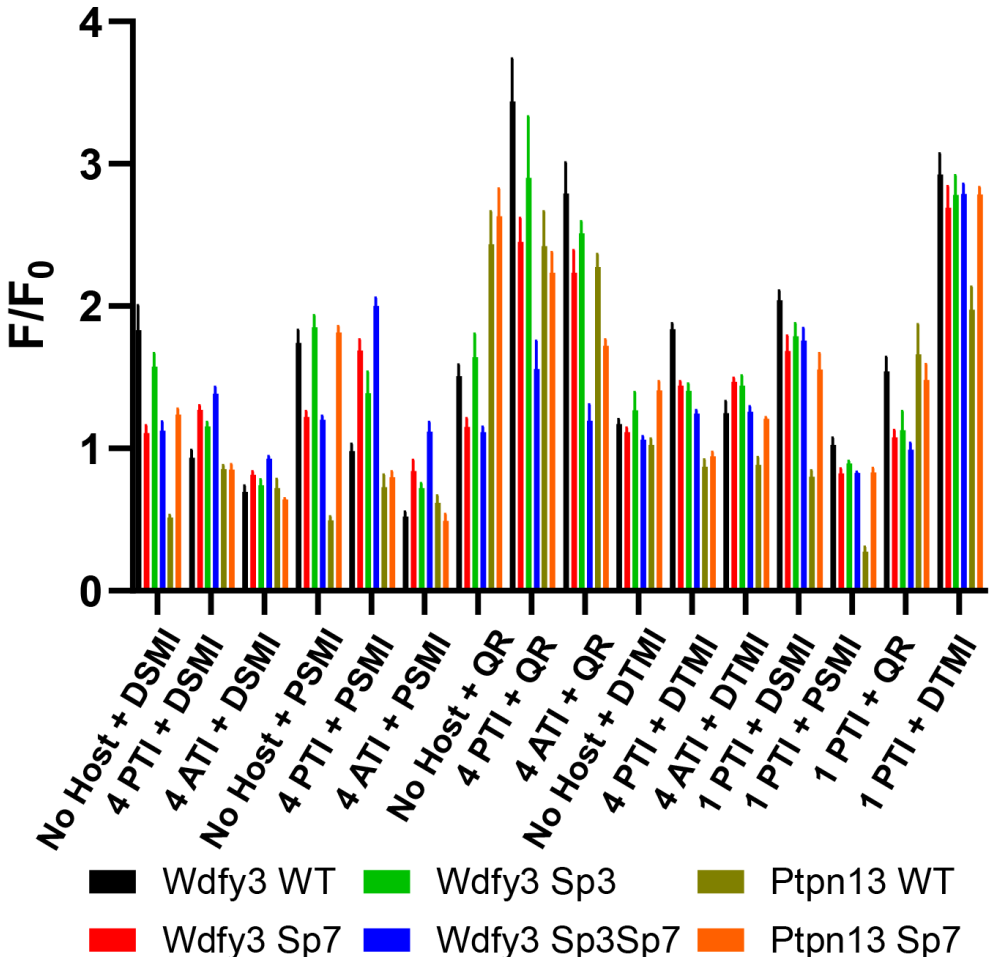

Figure S-40. Bar plots showing the F/F_0 that was generated for 16 elements: No Host + 0.5 µM **DSMI**, 4 µM **PTI** + 0.5 µM **DSMI**, 4 µM **ATI** + 0.5 µM **DSMI**, No Host + 0.5 µM **PSMI**, 4 µM **PTI** + 0.5 µM **PSMI**, 4 µM **ATI** + 0.5 µM **PSMI**, No Host + 0.5 µM **QR,** 4 µM **PTI** + 0.5 µM **QR**, 4 µM **ATI** + 0.5 µM **QR**, No Host + 0.5 µM **DTMI** 4 µM **PTI** + 0.5 µM **DTMI**, 4 µM **ATI** + 0.5 µM **DTMI, 1** µM **PTI** + 0.5 µM **DSMI**, 1 µM **PTI** + 0.5 µM **PSMI**, 1 µM **PTI** + 0.5 µM **QR**, and 1 µM **PTI** + 0.5 µM **DTMI**.

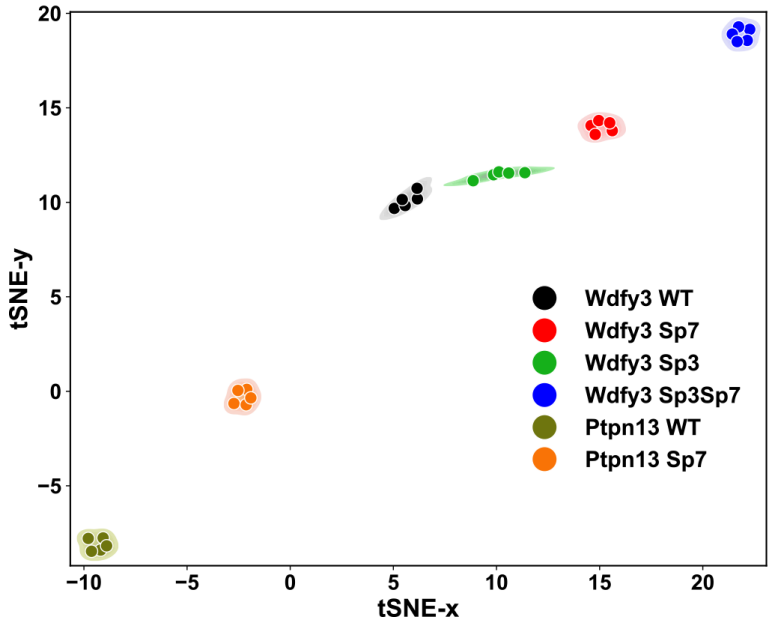

Figure S-41. t-SNE visualization with density estimation for differentiating four Wdfy3 peptides (WT, Sp7, Sp3, and Sp3Sp7) and two Ptpn13 peptides (WT and Sp7) of 16 elements (No Host + 0.5 μM **DSMI**, 4 μM **PTI** + 0.5 μM **DSMI**, 4 μM **ATI** + 0.5 μM **DSMI**, No Host + 0.5 μM **PSMI**, 4 μM **PTI** + 0.5 μM **PSMI**, 4 μM **ATI** + 0.5 μM **PSMI**, No Host + 0.5 μM **QR,** 4 μM **PTI** + 0.5 μM **QR**, 4 μM **ATI** + 0.5 μM **QR**, No Host + 0.5 μM **DTMI** 4 μM **PTI** + 0.5 μM **DTMI**, 4 μM **ATI** + 0.5 μM **DTMI, 1** μM **PTI** + 0.5 μM **DSMI**, 1 μM **PTI** + 0.5 μM **PSMI**, 1 μM **PTI** + 0.5 μM **QR**, and 1 μM **PTI** + 0.5 μM **DTMI**).

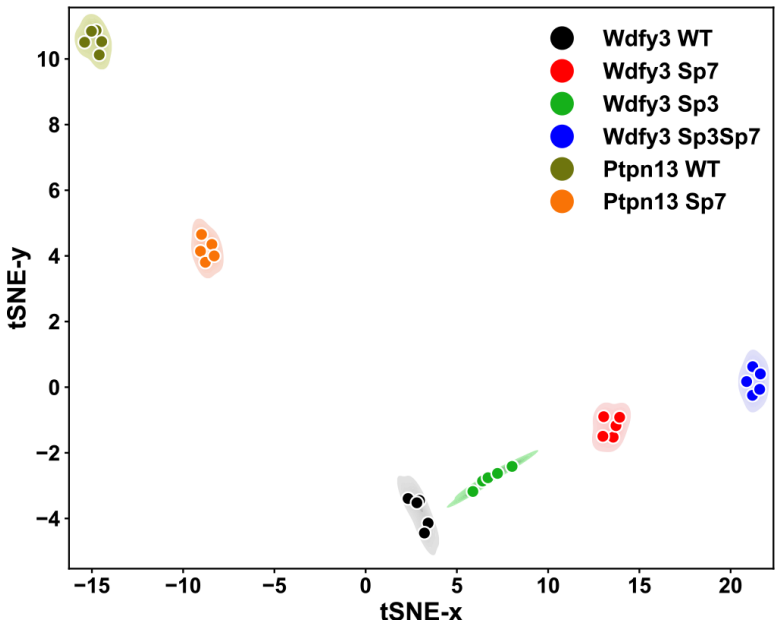

Figure S-42. t-SNE visualization with density estimation for differentiating four Wdfy3 peptides (WT, Sp7, Sp3, and Sp3Sp7) and two Ptpn13 peptides (WT and Sp7) of 12 elements (No Host + 0.5 μM **DSMI**, 4 μM **PTI** + 0.5 μM **DSMI**, 4 μM **ATI** + 0.5 μM **DSMI**, No Host + 0.5 μM **PSMI**, 4 μM **PTI** + 0.5 μM **PSMI**, 4 μM **ATI** + 0.5 μM **PSMI**, No Host + 0.5 μM **QR,** 4 μM **PTI** + 0.5 μM **QR**, 4 μM **ATI** + 0.5 μM **QR**, No Host + 0.5 μM **DTMI** 4 μM **PTI** + 0.5 μM **DTMI**, 4 μM **ATI** + 0.5 μM **DTMI**).

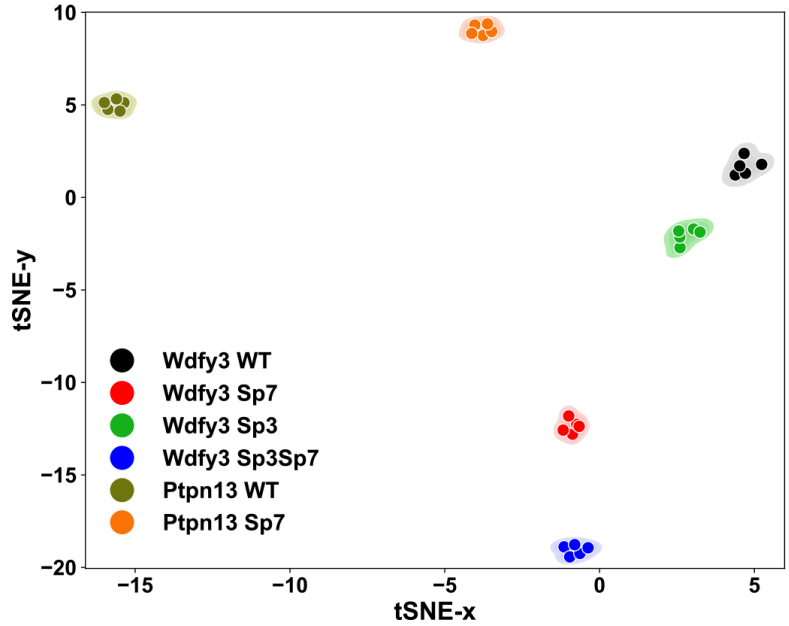

Figure S-43. t-SNE visualization with density estimation for differentiating four Wdfy3 peptides (WT, Sp7, Sp3, and Sp3Sp7) and two Ptpn13 peptides (WT and Sp7) of optimized 5 elements (No Host + 0.5 µM **DSMI**, No Host + 0.5 µM **PSMI**, 4 µM **PTI** + 0.5 µM **DSMI,** 4 µM **PTI** + 0.5 µM **PSMI**, and 4 µM **ATI** + 0.5 µM **QR**).

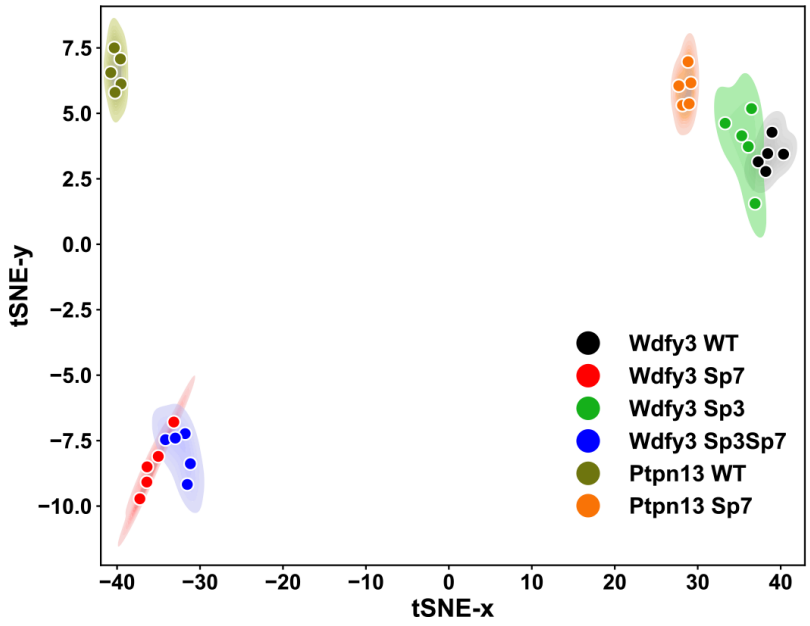

Figure S-44. t-SNE visualization with density estimation for differentiating four Wdfy3 peptides (WT, Sp7, Sp3, and Sp3Sp7) and two Ptpn13 peptides (WT and Sp7) of 0.5 µM **dye only** (**DSMI**, **PSMI**, **QR**, and **DTMI**).

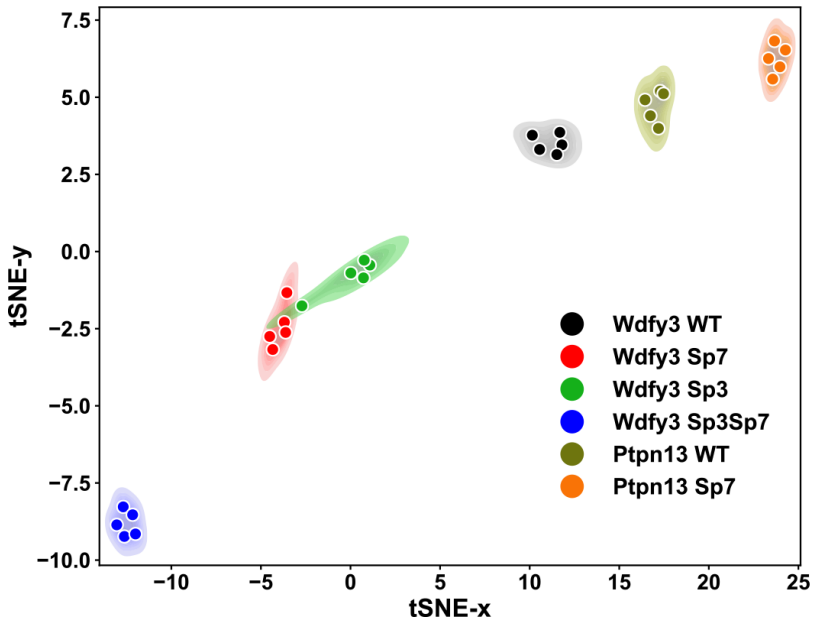

Figure S-45. t-SNE visualization with density estimation for differentiating four Wdfy3 peptides (WT, Sp7, Sp3, and Sp3Sp7) and two Ptpn13 peptides (WT and Sp7) of 3 elements (4 μM **PTI** + 0.5 μM **DSMI,** 4 μM **PTI** + 0.5 μM **PSMI**, and 4 μM **ATI** + 0.5 μM **QR**).

6. References

1. Y. Liu, M. Mettry, A. D. Gill, L. Perez, W. Zhong and R. J. Hooley, *Anal. Chem*., 2017, **89**, 11113–11121.
2. J. Chen, A. D. Gill, B. L. Hickey, Z. Gao, X. Cui, R. J. Hooley and W. Zhong, *J. Am. Chem. Soc*., 2021, **143**, 12791–12799.
3. A. D. Gill, B. L. Hickey, S. Wang, M. Xue, W. Zhong and R. J. Hooley, *Chem. Commun*., 2019, **55**, 13259–13262.
4. J. Chen, B. L. Hickey, Z. Gao, A. A. P. Raz, R. J. Hooley and W. Zhong, *ACS Sens*., 2022, **7**, 2164–2169.
5. B. L. Hickey, J. Chen, Y. Zou, A. D. Gill, W. Zhong, J. G. Millar and R. J. Hooley, *Chem. Commun*., 2021, **57**, 13341–13344.
6. Z. Fu, J. Lin, C. Li, W. Yan and T. Wu, *Cryst. Growth Des*., 2016, **16**, 2322–2327.
7. R. Subiros-Funosas, R. Prohens, R. Barbas, A. El-Faham and F. A. Albericio, *Chem. Eur. J*., 2009, **15**, 9394–9403.
8. SAINT, V8.30A, Bruker Analytical X-Ray Systems, Madison, WI, 2012.
9. SADABS, 2.03, Bruker Analytical X-Ray Systems, Madison, WI, 2016.
10. G. M. Sheldrick, *Acta Cryst. A*, 2008, **64**, 112–122.
11. G. M. Sheldrick, *Acta Cryst. A,* 2015*,* **A71**, 3-8.
12. O. V. Dolomanov, L. J. Bourhis, R. J. Gildea, J. A. K. Howard and H. Puschmann, *J. Appl. Crystallogr*., 2009, **42**, 339–341.
13. www.supramolecular.org.
14. S. U. Maier, A. B. Makwana and T. A. Hare, *Neuron*., 2015, **87**, 621–631.
15. J. Wang, R. M. Wolf, J. W. Caldwell, P. A. Kollman and D. A. Case, *J. Comput. Chem.,* 2004, **25**, 1157–1174.
16. A. Jakalian, D. B. Jack and C. I. Bayly, *J. Comput. Chem.,* 2002, **23**, 1623–1641.
17. J. Chen, C. L. Brooks and J. Khandogin, *Curr. Opin. Struct. Biol*., 2008, **18**, 140–148.
18. D. H. Herce, T. Darden and C. Sagui, *J. Chem. Phys*., 2003, **119**, 7621–7632.
19. P. Fasihianfard, K. Y. Wu, S. Kaushik and C.-A. Chang, *J. Phys. Chem. B*., 2025, **129**, 11168-11182.
20. D. R. Roe and T. E. Cheatham, *J. Chem. Theory Comput.,* 2013, **9**, 3084–3095.
21. B. R. Miller, T. D. McGee, J. M. Swails, N. Homeyer, H. Gohlke and A. E. Roitberg, *J. Chem. Theory Comput*., 2012*,* **8**, 3314–3321.
22. J. Kyte and R. F. Doolittle, *J Mol Biol.*, 1982, **157***,* 105–32.